

A FRAMEWORK FOR IMPLEMENTATION AND EVALUATION OF
COOPERATIVE DIVERSITY IN SOFTWARE-DEFINED RADIO

A Thesis

Submitted to the Graduate School
of the University of Notre Dame
in Partial Fulfillment of the Requirements
for the Degree of

Master of Science in Electrical Engineering

by

Glenn J. Bradford

J. Nicholas Laneman, Director

Graduate Program in Electrical Engineering

Notre Dame, Indiana

December 2008

A FRAMEWORK FOR IMPLEMENTATION AND EVALUATION OF COOPERATIVE DIVERSITY IN SOFTWARE-DEFINED RADIO

Abstract

by

Glenn J. Bradford

Increasing data rates in wireless devices is particularly challenging due to the presence of many impairments in the medium, including multipath fading. Diversity techniques are a means of increasing transmission reliability in multipath environments. This thesis focuses on cooperative diversity, a concept that obtains spatial diversity via relaying. Cooperative diversity encompasses a broad range of issues, from the physical layer through network layer, making the emerging reconfigurable technology of software-defined radio ideal for experimentation.

The main contribution of this work is the development of an extendable experimental framework for implementation and analysis of cooperative protocols. A decode-and-forward (DF) relay network is constructed and analyzed by means of received symbol distributions and bit error rate (BER) versus signal-to-noise ratio (SNR) curves. The former shows a shift in the distribution of instantaneous SNR for both simple and selective DF, while the latter indicates that only the selective scheme actually achieves a diversity gain.

To my family...
Mom, Dad, and Colleen.
The greatest gifts in my life.

CONTENTS

FIGURES	v
TABLES	vii
ACKNOWLEDGMENTS	viii
CHAPTER 1: INTRODUCTION	1
CHAPTER 2: BACKGROUND	5
2.1 The Wireless Fading Channel	5
2.2 Diversity	7
2.3 Cooperative Diversity	11
2.3.1 Theory	11
2.3.2 Implementations	12
2.4 Software-Defined Radio	13
2.4.1 The “Ideal” Software-Defined Radio	14
2.4.2 Hardware and Software Considerations	15
2.4.3 GNU Radio and the USRP	17
2.5 Summary	19
CHAPTER 3: A DECODE-AND-FORWARD RELAY NETWORK	20
3.1 Experimental Setup and Calibration	20
3.1.1 Apparatus and Geometry	21
3.1.2 Radio Nodes and System Parameters	23
3.1.3 Transmit Power Calibration	25
3.1.4 Channel Characterization	26
3.2 Software Description	29
3.2.1 Medium Access Control	31
3.2.2 Source Node	33
3.2.3 Relay Node	33
3.2.4 Destination Node	36
3.3 Summary	37

CHAPTER 4: RECEIVED SYMBOL DISTRIBUTION EXPERIMENT . . .	39
4.1 Theoretical Basis	39
4.1.1 Direct Transmission	39
4.1.2 Simple Decode-and-Forward Relaying	42
4.1.3 Direct and Diversity Comparison	46
4.2 Experimental Results	52
4.3 Summary	53
 CHAPTER 5: BER CURVE EXPERIMENT	 54
5.1 Theoretical Considerations	54
5.2 Simulation of BER for DBPSK System	55
5.3 Simple Decode-and-Forward Experimental Results	58
5.4 Selective Decode-and-Forward Results	60
5.5 Summary	64
 CHAPTER 6: CONCLUSIONS AND FUTURE WORK	 65
6.1 Conclusions	65
6.2 Future Work	66
 BIBLIOGRAPHY	 68

FIGURES

1.1	Three node cooperative diversity example	2
2.1	BER versus SNR in the high SNR regime for no diversity (L=1) and diversity order 2 (L=2) with coding gain $c=1$	10
2.2	Block diagram for an “ideal” software-defined radio	14
3.1	Experimental setup	22
3.2	Probability of error versus SNR for DBPSK in Rayleigh (K=0) and Rician (K=10) fading	27
3.3	Histograms of channel strength and its approximate distribution for experimental setup (a) without shielding and (b) with shielding	28
3.4	Probability of error versus SNR for DBPSK in Rayleigh (K=0) and Rician (K=1.05) fading	29
3.5	Code dependencies for BER experiment	30
3.6	Flow diagram for BER experiment	32
3.7	Block diagrams of decode-and-forward relay network nodes	34
3.8	Hierarchical blocks for DBPSK decode-and-forward relay implementation	35
4.1	Probabilistic model for three node decode-and-forward relay network	43
4.2	Probability distributions of received symbols for direct transmission, simple DF, and transmit diversity	46
4.3	Probability distribution of received symbols for direct transmission for different values of average SNR	48
4.4	Probability distributions of received symbols for direct, simple DF, and transmit diversity left of the origin	49
4.5	Histograms of received symbols for simulated DBPSK direct and simple DF relay transmission	51

4.6	Histograms of received symbols for experimental DBPSK direct and simple DF relay transmission	52
5.1	Simulation of BER versus SNR for three node decode-and-forward relay network for various transmission schemes	57
5.2	BER versus transmit power for three individual links in simple DF relay network	59
5.3	BER versus transmit power for direct and diversity paths in simple DF relay network	60
5.4	BER versus transmit power for three individual links in selective DF relay network	62
5.5	BER versus SNR for direct and diversity paths in selective DF relay network	63

TABLES

3.1	SYSTEM PARAMETERS	24
-----	-----------------------------	----

ACKNOWLEDGMENTS

Naturally, I am indebted to many people for getting me to the point I am today. Many thanks to my advisor, Dr. J. Nicholas Laneman, for his support, guidance, and example through this entire process. Also, thanks to all those in my research group and department who have been generous in offering help and advice to me. Brian Dunn, Michael Dickens, Matthieu Bloch, Neil Dodson, and Ralf Bendlin just to name a few.

A special thanks to Corneilus Griggs for assistance in constructing my experimental setup. I should also acknowledge all those who maintain and contribute to the GNU Radio software project. Though I do not know most of these people, this work would not have been possible without their efforts.

Thanks to all my friends who make life enjoyable. Finally, thanks to my family. My sister for her laughter. My father for his friendship. And my mother for her sheer dedication.

CHAPTER 1

INTRODUCTION

As the demand for data-intensive applications for mobile devices continues to grow, understanding and exploiting the wireless propagation environment is of paramount importance. Consequently, much energy has been invested in researching wireless data transmission. Although the wireless channel is in many ways similar to its relative the wired communication channel, there are many phenomena observed in the wireless channel that are either not present or are less pronounced in the wired channel. These impairments make reliable communication over the wireless channel at high data rates particularly challenging.

One impairment that can become particularly severe is multipath fading. It results from a transmitted signal arriving at a destination via multiple and typically independent paths. The destination sees a superposition of multiple copies of the signal, each of which has a magnitude and phase dependent on the distance and geometry of the path it followed. If the phases of the replica signals all have similar values, they will add constructively at the destination, producing a stronger than expected signal given the distance between the nodes. Unfortunately, if the replicas are out of phase, destructive interference occurs, producing a weaker signal. Node movement or changes in the environment will alter the geometry and number of paths over which the signal reaches the destination, effectively making the received signal strength vary drastically with time and frequency. It has been observed in

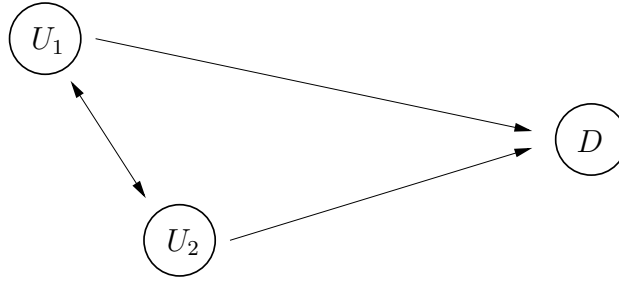


Figure 1.1: Three node cooperative diversity example

wireless channels suffering from multipath fading that the bit error rate (BER) decays much slower with increasing signal-to-noise ratio (SNR) as compared with the additive white Gaussian noise (AWGN) channel. This is a direct result of the fluctuation of instantaneous SNR induced by multipath fading, and leads to a decrease in the reliability of transmission.

Cooperative diversity [1, 2, 3] has generated a great deal of interest as a method for both increasing reliability and data throughput in wireless mediums. In its simplest form, cooperative diversity encompasses wireless nodes relaying the signals of other nodes on to their respective destinations. With multiple copies of the same message, the destination can decode with greater accuracy the message sent from a given source, even if severe channel impairments are present in a subset of the channels. Figure 1.1 depicts a scenario in which two users, U_1 and U_2 , each have information they wish to transmit cooperatively to a common destination D . Each node is able to listen to the message broadcast by its counterpart and either repeat this message or some information about it on to the destination. At the destination, the multiple copies of each source's message are used to decode the original message, enabling the destination to, hopefully, average over independent instantaneous channel realizations, increasing the reliability of transmission and the

rate at which the BER decreases with increasing average SNR.

Because cooperative diversity can involve the cooperation of many distinct nodes within a given network, it motivates a creative rethinking of the definitions and interactions of the physical, link, and network layers of the network protocol stack [4]. In order to perform experimentation across these layers, a highly flexible hardware architecture is desirable. The concept of software-defined radio (SDR) [5] is another topic of considerable recent interest whose goal is to perform signal processing not in fixed hardware, but rather in highly reconfigurable devices, such as field-programmable gate arrays (FPGA), digital signal processors (DSP), and general purpose processors (GPP). This approach makes communication systems' product development faster and dynamic reconfiguration possible. The highly flexible nature of SDR makes it an ideal infrastructure on which to experiment with cooperative diversity protocols.

The primary contribution of this work is the basis for an experimental network to practically evaluate different cooperative communication architectures. It is an experimental setup built using open source SDR software and hardware, making it possible for others to take advantage of the functionality implemented. This thesis highlights a number of implementation issues that must be taken into account when developing real-world cooperative diversity networks, specifically in SDR but also in more general hardware. To analyze the diversity gain provided by certain cooperative protocols implemented on this setup, this work looks at both the experimental distribution of received symbols and BER versus SNR curves. Rationale for looking at received symbols is given along with an explanation of why it cannot definitively prove the presence of diversity but can show an underlying shift in the instantaneous SNR distribution, which is necessary for diversity. This metric, though considerably less informative than BER behavior, is simpler to obtain

experimentally. Experimental BER versus SNR curves indicate a diversity gain for selective decode-and-forward, in which the relay does not forward packets containing errors, but not for simple decode-and-forward, where the relay does forward packets containing errors.

The remainder of this thesis is organized as follows. Chapter 2 provides more background and literature references for the concepts of cooperative diversity and SDR. Chapter 3 describes the design choices and development of the experimental system. Chapter 4 gives rationale for the use of the received symbol distribution as a metric for detecting diversity along with experimental results using this metric. Chapter 5 provides results for the experimental setup using the comparison of BER versus SNR curves for both simple and selective decode-and-forward transmission. Finally, Chapter 6 draws some overall conclusions and outlines directions of future research. All code used for experimentation can be found with the electronically archived version of this thesis, available at [6].

CHAPTER 2

BACKGROUND

This chapter gives a more thorough exploration of cooperative diversity, SDR, and related topics. The topics of the wireless fading channel, diversity, cooperative diversity, and SDR are addressed. Relevant literature and tutorials are referenced for the reader's aid.

2.1 The Wireless Fading Channel

An introductory treatment of the wireless channel, its impairments, and methods for combatting these impairments can be found in [7]. Impairments in the wireless channel are generally classified into two groups: small-scale and large-scale effects, referring to the time and spatial scale over which the degradation of the channel varies. Large-scale phenomena include effects such as path loss and shadowing, small-scale phenomena include multipath fading.

Path loss is a result of the transmitted power of a signal being spread over an ever greater surface area as it propagates farther from a source. In free space, this surface area would be a sphere, leading received power to decrease proportionally with d^2 , where d is the distance from the transmitter to the receiver. Real-world wireless devices do not operate in free space, resulting in signal energy being absorbed by objects between the transmitter and receiver, commonly termed shadowing. Shadowing and path loss are often combined in modeling as a decay of signal power with

distance proportional to d^α , where $\alpha > 2$. The path loss exponent depends upon the density of objects in the environment.

A small-scale effect whose mitigation is the focus of this thesis, multipath fading can be severe depending on the particular channel. Multipath fading, which will also be referred to simply as fading in this work, occurs when radio nodes are in an environment with multipath signal propagation and there is either node movement or variation in the nodes' surroundings. Multipath propagation refers to a transmitted signal arriving at a destination via multiple paths, causing the destination to see a superposition of copies of the same signal, each of which has a magnitude and phase dependent on the distance and geometry of the path it followed. If the transmitter or receiver are moving in their environment or there are changes to the environment, then the magnitude and phase of each signal replica will vary with time, creating a fluctuation in the overall magnitude and phase of the received signal.

This fluctuation is multipath fading, and it makes reception difficult, for the channel can be strong at one moment and severely degraded the next. When the channel degrades so severely that transmission becomes unreliable or impossible, the channel is said to be in a deep fade. Some important quantifications of the multipath fading channel are:

- delay spread – time difference between first and last arriving signal copies
- Doppler spread – range of observed frequencies due to the movement of nodes
- coherence time – time scale at which channel realizations are roughly independent
- coherence distance – typical distance that a node must move to produce an independent channel realization
- coherence bandwidth – the range of contiguous frequencies that experience essentially the same multipath fading effect

Since characterizing each configuration of radio nodes within a physical environment to determine the exact multipath fading model is prohibitively complex,

most literature on multipath assumes a probabilistic model. If the delay spread of the multipath is less than a symbol period, a single tap finite impulse response (FIR) filter is common for modeling the effect of multipath. This filter will have a flat frequency response, affecting all frequencies equally. For the treatment of frequency selective fading, see [7]. The typical discrete-time, baseband model used for a received symbol is

$$r[m] = h[m]s[m] + w[m] \quad (2.1)$$

where s is the transmitted symbol at time m , r the received symbol, and w models thermal noise as a complex Gaussian random variable with zero-mean and variance $N_0/2$ per dimension. The fading is modeled by the random multiplicative term h . If a line-of-sight path does not dominate the spectral paths, a Rayleigh fading model specifies h as a zero-mean, complex Gaussian random variable, the magnitude of which is Rayleigh distributed, the squared magnitude of which is exponentially distributed. Rician fading adds a direct path term with random phase to account for a strong line-of-sight path. This thesis will assume a slow-fading model corresponding to the symbol period being much smaller than the coherence time, allowing the time index of h to be ignored. If the magnitude of h is small, the effective result is to reduce the instantaneous received signal strength. In this scenario, even with a high transmit power, the receiver can see a reduction in noise immunity and make more errors in detection.

2.2 Diversity

Diversity is an attempt to increase transmission reliability in the fading environment via transmitting data from a source to a destination in multiple forms over, ideally, multiple independent fading realizations. The motivation for such an approach stems from the fact that, even if it is highly probable one path is in a deep

fade, it is less likely all paths will be severely impaired, providing robustness against multipath fading. Common forms of diversity include time, frequency, and space diversity.

The simplest form of time diversity is to repeat a symbol over multiple symbol intervals, also called repetition coding. Intervals must be spaced such that independent realizations of the channel occur. Time diversity introduces a decoding delay at the receiver, since it must wait for all copies of the signal to arrive before decoding can proceed. Frequency diversity is possible when the signal bandwidth is greater than the coherence bandwidth of the channel. Although some frequencies of the signal will be severely attenuated, others will not be. Communication schemes such as code division multiple access (CDMA) and orthogonal frequency division multiplexing (OFDM) can take advantage of frequency diversity.

Spatial diversity comes in a variety of forms. Transmit diversity can be created by using multiple transmit antennas with a single receive antenna; receive diversity can be created by using multiple receive antennas with a single transmit antenna. A combination of the two results in a multiple-input multiple-output (MIMO) system. For diversity gains, paths between different antenna pairs must be independent. This can usually be achieved by separating the collocated antennas by at least half of a wavelength of the carrier. Even without independent paths, multiple receive antennas give a power gain by capturing more of the transmitted power.

For the AWGN channel model,

$$r[m] = s[m] + w[m] \tag{2.2}$$

where n is Gaussian, the signal to noise ratio (SNR) is defined as

$$\text{SNR} = \frac{\mathbb{E}[ss^*]}{\mathbb{E}[ww^*]} \tag{2.3}$$

$$= \frac{P}{N} \tag{2.4}$$

where $\mathbb{E}[\cdot]$ is the expectation, P is the transmitted power, and N the noise power. A common way of assessing performance for a given transmission scheme over the AWGN channel is to look at how quickly the bit error rate (BER) decreases with SNR. The rest of this thesis assumes a binary alphabet with $s \in \{-a, a\}$, meaning that the symbol error rate (SER) and BER are interchangeable. BER is known to decrease with the square of SNR for the AWGN channel when plotted on a log-log scale [7]. In fading channels, it has been observed that the BER only decreases at a rate proportional to the inverse of SNR. This represents considerably worse performance than in the Gaussian case.

The BER of diversity schemes can be approximated in the high SNR regime as [7]

$$\text{BER} \approx (c \cdot \text{SNR})^{-L} \quad (2.5)$$

where L is known as the diversity order and determines the rate at which the probability of error or BER decays at high SNR. Additionally, c is a coding gain obtained when codes more efficient than repetition coding are employed. Figure 2.1 compares the BER versus SNR curves for systems both with and without diversity using a log-log scale. The BER of the system with diversity can be seen to decay linearly at a rate of two orders of magnitude per decade of SNR. This steeper slope is characteristic of diversity schemes. The rate at which it decays is equal to the diversity order and is typically the number of independent paths in the system.

Observing or proving the presence of diversity is thus usually done by means of BER curve analysis. This is a natural choice since it not only indicates the presence of diversity, but actually is a measure of the gain obtained therefrom. For an information theoretic observance of diversity, outage probability behaves in a similar fashion to BER [7].

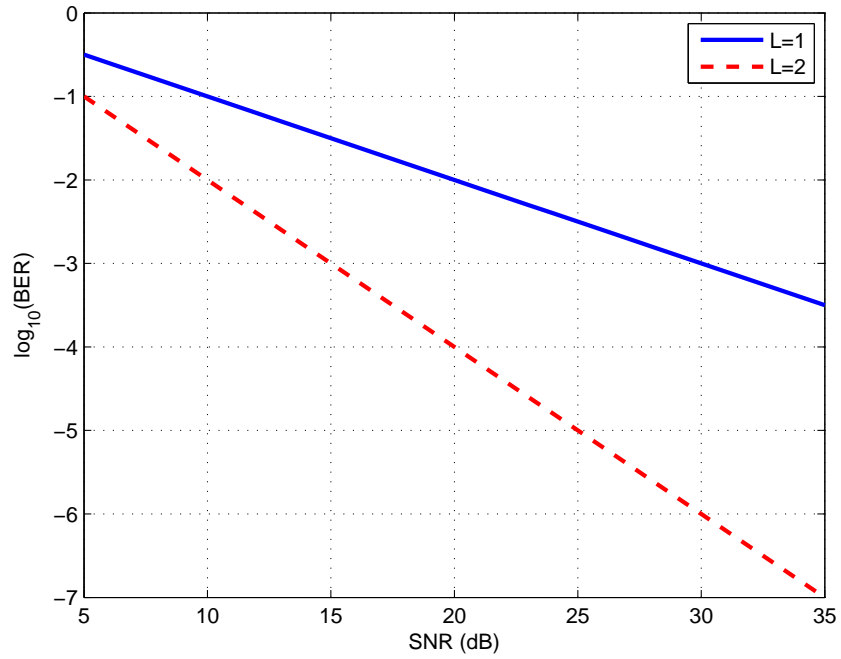


Figure 2.1: BER versus SNR in the high SNR regime for no diversity ($L=1$) and diversity order 2 ($L=2$) with coding gain $c=1$

2.3 Cooperative Diversity

2.3.1 Theory

Although many base stations employ multiple antennas in order to create spatial diversity, the size of the typical handset or mobile device precludes this possibility. The antennas cannot be placed far enough apart to create independent paths. Cooperative diversity [1, 2, 3] is an attempt to extend the spatial diversity gains experienced by MIMO systems to size-constrained mobile devices through relaying. This is accomplished by nodes within a network listening to each other's messages and relaying these messages on to their intended destination, hence classical works on the relay channel are relevant [8]. Since the wireless medium is broadcast in nature, there is "no cost, in terms of transmit power," [1] in sending a copy of the message from a source to a cooperating node. Each user can listen to the other user's message and forward either its estimate of the message or some other information about it on to the destination. Ideally, the destination ends up with multiple, independently faded copies of the same message, providing diversity to combat channel degradation.

The amount of cooperation each node performs can be varied, leading to a classical relaying scheme in the degenerate case of one node having no information of its own to send. Cooperative diversity comes at the cost of spectral efficiency [3]. Nodes spend time and power relaying each other's messages rather than new information. For cooperative diversity to be a useful concept, the spatial diversity gains it produces must outweigh the loss of spectral efficiency. Diversity results in a lower required SNR (and thus less transmit power) for a given probability of error. This power can either be saved or used to regain the lost spectral efficiency by transmitting with a larger symbol constellation. In addition to countering multipath fading, cooperative diversity can also help mitigate path loss and shadowing effects.

In [1, 2], the authors look at a general case of cooperation and then numerically analyze a CDMA implementation of what they term *User Cooperation*. They show that, for their proposed system, cooperation brings benefits in the forms of increased throughput and cell coverage, and decreased channel variation sensitivity.

A close examination of cooperation in slow fading environments is provided in [3]. The half-duplex constraint of practical radios is taken into account by nodes transmitting on time orthogonal channels, though the orthogonality of channels need not be obtained by time division multiple access. Additionally, channel state information (CSI) is assumed only to be available at the receivers. A host of diversity schemes are discussed including amplify-and-forward (AF), decode-and-forward (DF), selection relaying, and incremental relaying. AF simply involves retransmitting samples of the received analog waveform. DF first makes decisions about what symbols were sent by the source before retransmitting these estimated symbols. Selection relaying only relays information if the inter-user channel is of a high enough quality to make it worthwhile. Incremental relaying is an attempt to regain spectral efficiency by only relaying when required, thus necessitating feedback from the destination. All schemes are shown to achieve full diversity except for DF.

2.3.2 Implementations

An early implementation example of cooperative diversity can be found in [9]. Simple, commodity hardware consisting of a microcontroller and radio unit were used to create cooperative relays. For experimental evaluation, weather data was transferred wirelessly from a computer to a display on the other side of the room. Multiple relays within the room used pilot tones from the source and destination to determine their overall channel quality. To ensure only the relay with the best channel cooperated, they were set to volunteer at a time delay inversely proportional

to their observed channel quality. The relay fully decoded the message and only forwarded if a cyclic redundancy check (CRC) on the packet was verified. The destination checked both copies of the received packet with the CRCs and selected the packet, if any, that had no errors. The benefits of diversity were observed qualitatively by noting that the display at the destination had noticeably fewer errors in the text when cooperation was employed.

A more quantitative analysis was performed in [10]. An amplify-and-forward network was constructed based on an OFDM physical layer and distributed Alamouti transmit diversity scheme using WARP, an FPGA based SDR developed at Rice University [11]. For evaluation, a three node network with the relay approximately halfway between the source and destination was set up. There was no mobility in the network and a line-of-sight path existed between all nodes. A plot of BER versus SNR shows that the cooperative scheme outperformed the non-cooperative scheme. No diversity gain is discernible in the graphs.

2.4 Software-Defined Radio

One key requirement for the implementation of cooperative communications is node flexibility and reconfigurability. Cooperating nodes must have the ability to dynamically change on which channels they transmit and receive in order to coordinate and assist other nodes. In addition to this, the traditional distinctions between layers in the network protocol stack become blurred. Knowing when to cooperate and with whom requires knowledge of the network topology, channel quality, and when to access the medium, information usually spread between the physical, link, and network layers. As such, cooperative diversity offers an opportunity to rethink and optimize across traditional protocol stack layers [4]. All of this serves to highlight the need for a flexible infrastructure on which to experiment with cooperative

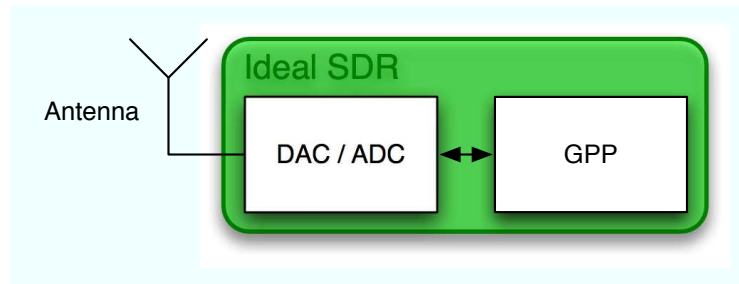


Figure 2.2: Block diagram for an “ideal” software-defined radio

schemes. SDR is an ideal technology on which to do so and possibly, one day, provide commercial products.

2.4.1 The “Ideal” Software-Defined Radio

The motivating goal of SDR is flexibility. Its aim is to provide quick development and easy reconfigurability in radios by implementing all signal processing in software. Explanations of the basic concept of SDR and some of the practical design considerations can be found in [5, 12]. A diagram of the “ideal” SDR is depicted in Fig. 2.2. The received analog signal on the antenna is sampled by an analog to digital converter (ADC) that captures the entire bandwidth of interest. These samples are then sent to a reconfigurable device such as a GPP, DSP, or FPGA where all filtering, rate and frequency conversion, and baseband processing are carried out. The transmit path is similar, only with a digital to analog converter (DAC) in place of the ADC.

By implementing signal processing, coding, and protocols in reconfigurable rather than fixed hardware, dynamic modifications to the radio become possible. New radio architectures can be developed simply by writing new software as opposed to changing the underlying hardware of the device. Such ability could enable devices

to be universal without needing separate hardware for every functionality desired. One can imagine a single product that could access mobile phone networks and WiFi access points, receive local and satellite radio stations, and display digital TV transmissions. Such flexibility also provides a means by which to manage the numerous, highly divergent protocols that govern current wireless communication systems. Dynamic reconfigurability also enables the development of “smart,” “cognitive” radios [13] capable of adapting to optimize performance for given conditions.

2.4.2 Hardware and Software Considerations

Unfortunately, the pure software radio is “an ideal that may never be fully implemented” [5]. Numerous limitations in current hardware preclude a single radio from operating in several or all of today’s commonly used radio frequencies. As a result, there is “an acknowledgement that some signal processing will continue to be done in RF circuitry” [12] and that reconfigurability may be required in hardware as well as software. Chief among the limitations is that current ADCs have neither the sampling rate to capture all possible frequencies of interest nor the dynamic range to simultaneously quantize signals of significantly different power levels. Performing signal processing at radio frequency (RF) or even at an intermediate frequency (IF) is computationally intensive even for the fastest of current GPPs. Functionalities that must be implemented at RF and IF are often assigned to a faster, reconfigurable hardware device, such as an FPGA.

As indicated above, although the goal of SDR is to do all development in software, hardware still plays a crucial role in what is and is not practical for a given SDR. Multiband antennas are needed that can receive signals over a wide range of frequencies with reasonable gains. Additionally, tunable RF circuitry is needed to filter the analog signal and shift it to IF before it is digitized by the ADC.

For processing the digital signal, there are a number of available reconfigurable devices, each with their own strengths and liabilities [14]. GPPs provide the greatest flexibility and ease of programming, but also the least in terms of performance. Recent increases in processor speed and the development of multicore processors are making computationally intensive signal processing in GPPs possible. Timing delays within a GPP, however, can be impossible to quantify deterministically. DSPs are essentially processors optimized for signal processing that perform better than GPPs, but are also more difficult to program. Greater parallelism and control over timing is offered by FPGAs, but this also makes them considerably harder to program. Finally, application specific integrated circuits (ASIC) are ICs specially designed to perform set signal manipulation. They are naturally the fastest of all the options, but their reconfigurability is limited to design time. ASICs are most appropriate for performing functions that are common to a wide range of algorithms.

Typically, current SDRs use a combination of these four hardware types in order to be effective. Computationally expensive processing, such as at IF, is usually done in an FPGA. This includes operations such as sample rate conversion and channelization, the task of selecting the desired channel(s) from the quantized band(s) and shifting to baseband [15]. Baseband processing is often done in the more easily programmed GPP or DSP, depending on how complex the processing is.

Many considerations factor into efficient signal processing in both software and reconfigurable hardware. Most importantly, signal processing must be implemented in as efficient a manner as possible, fully using available resources such as multicore processors. SDRs will benefit greatly from the growing interest in effective multicore programming that is really just in its infancy. Related to this, managing different processor types within a single device can be complex. A hardware abstraction layer would allow an SDR to “avoid complexity, provide flexibility and improve portability

and code reusability” [16]. Rather than seeing various different hardware types, an application programmer would see only one virtual device, allowing programming for multiple architectures to be done concurrently. The abstraction layer would take care of deciding what hardware is best suited for a given operation or function.

As can be seen, SDRs can provide flexibility on a range of levels dependent on hardware selection. While an “ideal” SDR is not possible at this time, current SDRs can still provide a large degree of reconfigurability.

2.4.3 GNU Radio and the USRP

GNU Radio [17] is an open source software package that allows signal processing to be done efficiently on a GPP. It is also the SDR system used for this thesis. When combined with some front end hardware, it allows an SDR to be implemented on a desktop, laptop, or embedded computer. GNU Radio has a sizeable community of support and has been installed on computers running Linux, Mac OS X, and Windows. Signal processing functionality is performed in blocks created with C++ [18], which can be tied together in a flow graph built in the Python programming language [19] to process data in a streaming manner. GNU Radio was chosen for the underlying system in this thesis because of the relative ease of programming a GPP for application development. The open nature of the project made it possible to leverage the work already done by others and provided an opportunity to add functionality of which others could easily take advantage. For more information about GNU Radio see [20]. Good tutorials for GNU Radio can be found at [21].

GNU Radio provides a means of efficiently manipulating digital data on a GPP, but a method of capturing an analog radio signal and transforming it to the digital domain is still needed. The standard hardware used for this in the GNU Radio world is Ettus Research’s Universal Software Radio Peripheral (USRP) [22, 23]. The

USRP consists of a base motherboard and daughterboards that can be interchanged to allow operation in different bands of the radio spectrum. These daughterboards are tunable to a degree, but ultimately the USRP solves the tunable RF front end requirement of SDR by providing modular hardware. Daughterboards come in transmitter, receiver, and transceiver varieties. They provide filtering of the received signal and conversion from RF to IF and vice-versa. Experiments for this thesis were performed with the FLEX400 daughterboard [24], which is a transceiver capable of operating in the 400 MHz to 500 MHz range with a peak output power of 100 mW. Independent local oscillators make it possible to transmit and receive on distinct frequencies.

Once the analog signal has been converted to IF by the attached daughterboard, it is sampled by an ADC before being converted to baseband by a digital downconverter (DDC) implemented in the onboard FPGA. The baseband digital signal is sent to the host computer running GNU Radio via USB. The transmission path is similar, but consists of digital upconverters (DUC) and a DAC.

The combination of the GNU Radio and the USRP has a number of limitations, including a timing delay and limit on the bandwidth of quantized signals, both imposed by the USB link, and the lack of true parallel processing in a GPP. Additionally, neither GNU Radio nor the USRP are extensively documented. Despite these factors, it did provide the required functionality and adequate performance for the implementation of a cooperative diversity scheme. Furthermore, the open source nature of these projects meant not having to start from scratch when designing the system and that work done could be expanded on by others.

2.5 Summary

This chapter provided a brief overview and literature references for the concepts of cooperative diversity and SDR. Multipath fading is a severe impairment often present in wireless channels that requires mitigation to achieve reliability. Diversity techniques are a way of counteracting multipath via the obtaining of independent channel realizations for averaging; cooperative diversity is one such technique that uses relaying by wireless nodes within a network to provide spatial diversity. The unique set of cross layer issues it raises makes reconfigurable hardware such as SDR, itself a rich area of research, an ideal candidate for experimentation.

CHAPTER 3

A DECODE-AND-FORWARD RELAY NETWORK

This chapter describes the physical setup, hardware components, and code used to implement a cooperative diversity algorithm in SDR. The goal of the implementation was to observe diversity gains in a real-world setting and to provide a framework for optimization of cooperative protocols in practical network environments. Subsequent chapters will describe the metrics used to ascertain the presence of diversity gains within the network. These metrics include comparing the BER curves of the cooperative scheme with direct transmission, which is a natural choice from the literature, and the closely related concept of comparing the received symbol distributions of the two schemes.

3.1 Experimental Setup and Calibration

For simplicity, the network was comprised of three nodes: a source node, a relay node, and a destination node. The relay fully decoded the source's message before forwarding it on to the destination which, while not guaranteed to provide full diversity, is one of the simplest schemes possible. This section will describe this simple network's geometry and system parameters. Steps taken for characterization of the network and calibration of the nodes will also be discussed.

3.1.1 Apparatus and Geometry

For the generation of BER curve data, the average received SNR for a given configuration must be known. This average received SNR is a factor of the path loss, and thus the distance that exists between two given nodes, and the transmit power. Estimating received SNR for a given channel realization at the destination is not helpful, as this includes the reduction in SNR resulting from attenuation of the signal by the multipath fading. There are two suitable ways of overcoming this difficulty: keeping the distances between the nodes fixed while varying transmit power in a known way, or keeping the transmit power fixed while varying the distances between the nodes in a known way. For simplicity, the former was adopted. The requirement to average over multiple realizations of the multipath channel gain means that the network nodes must also be moved within their environment.

These requirements led to the experimental apparatus seen in Fig. 3.1. The three nodes in the relay network are fixed to the corners of an equilateral triangle. The distance between nodes on the triangle is adjustable between 2 m and 3 m. Wheels are attached to the bottom of the triangle, and power and USB wires are routed on the sides to allow for easy movement of the experiment. The equilateral triangle results in equal average received SNR for the source-destination (S-D) link, the source-relay (S-R) link, and the relay-destination (R-D) link. In this setup, the average relay path (S-R-D) will not have an advantage over the direct path (S-D).

It is desirable for the receive antennas to be located in the far-field antenna pattern of the transmitting antennas. In this region, signal strength is dependent solely on the distance from the transmitter and not on angular position. A general rule-of-thumb [25] that can be used for determining where the far-field begins is

$$d_{ff} = \frac{\lambda}{2\pi} \tag{3.1}$$

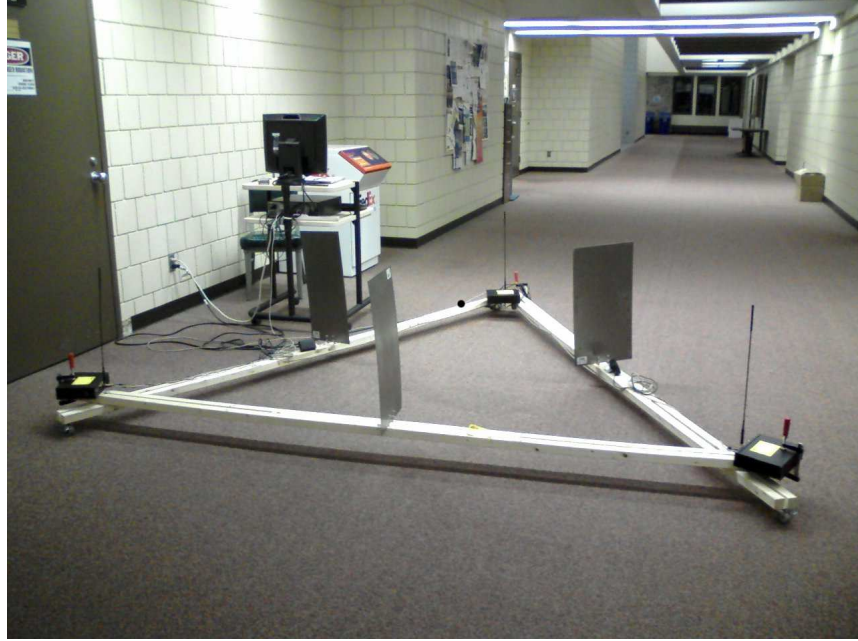


Figure 3.1: Experimental setup

where λ is the wavelength of the signal. For this experiment with a carrier frequency of 450 MHz, λ was 0.67 m, giving an d_{ff} of 0.11 m. Again, a rough estimate [7] for the coherence distance is

$$d_c = \frac{\lambda}{4} \quad (3.2)$$

which for this carrier frequency is 0.17 m. In order to obtain independent multipath gains, the nodes need to be moved by approximately this distance.

During experimentation, the triangle was pivoted back and forth in a half arc about one corner. Since at least one node in each link was moving, all channel gains varied. The length of the arc was 3.43 m, larger than the coherence distance of the carrier frequency to ensure independent channel realizations were obtained. Nodes moved at approximately 0.27 m/s, making the coherence time about 1.23 s. Based on the transmission rate used of 50 kbps and the packet length of 500 bytes (4000

bits or symbols), the coherence time is much greater than the transmission time of a packet, creating a slow fading environment in which all symbols within a packet experience approximately the same fading. Additionally, 1 ft x 2 ft metal sheets were placed in the middle of each radio link to attenuate the line-of-sight path. A discussion about the difficulties created by a strong line-of-sight path when trying to observe diversity as well as characterization of the channels in this experimental setup can be found in Sec. 3.1.4.

3.1.2 Radio Nodes and System Parameters

For each of the three radio nodes in the network, USRPs with FLEX400 daughterboards were used, making transmission possible in the 400 MHz to 500 MHz band. Rather than having a separate computer for each node, one central computer was used to perform the baseband processing of all three nodes. The central control of all nodes made it simple to create a time division multiplexing (TDM) scheme in which access to the medium by different nodes was guaranteed not to overlap. Transmit power was controlled through scaling the amplitude of the digital signal sent to the hardware for conversion to analog. This amplifier functionality was used to estimate BERs for various transmit powers.

It is somewhat artificial to have one single entity controlling all three nodes within the network. In a real application, the software for each node would be distributed and running on separate hardware at each node. Running all nodes on a single computer increases the burden on the computer's resources; this bottleneck effectively limited the rate at which data could be sent.

Control was centralized to simplify a number of implementation issues for the experiments. The transmitted packet and received packets at each node could be easily compared with one another to determine in real-time the number of errors

TABLE 3.1

SYSTEM PARAMETERS

System	Value	Carrier/Timing Recovery	Value
Modulation	DBPSK	Costas alpha	0.15
Bit rate	50 kbps	Costas beta	0.00562
Baseband sampling rate	250 kS/s	Mu	0.5
Hardware interpolation	512	Mu gain	0.1
Hardware decimation	256	Omega	5
Pulse shape	RRC	Omega gain	0.0025
Roll off	0.35	Omega relative	0.01
Bandwidth	67.5 kHz	fmin	-0.025
Access code size	8 Bytes	fmax	0.025
Packet number size	2 Bytes		

that occurred. This comparison in real-time eliminated the need to save data and compare after experimentation. It was also apparent when a packet was missed at a particular node, ensuring that packets were only compared when they corresponded to the same transmitted packet. The packet numbers could also have been used for this purpose, but the possibility of corruption of packet numbers complicated this approach. In short, centralized control was the simplest method of avoiding the necessity of more robust and complicated methods of ensuring data reliability, which are typically implemented at higher layers in the protocol stack.

A summary of system parameters used in experimentation can be found in Table 3.1. The modulation format used was differential binary phase shift keying (DBPSK) in which information is carried by the change in phase of the transmitted symbols. Though differential encoding and decoding do not require phase coherence between the destination and source, carrier frequency offset can be problematic. As a result, a Costas loop was used for both phase and frequency correction.

Because a single USB interface and processor bore the communication and baseband processing load for all three nodes, the data rate was conservatively set at 50 kbps. The typical current computer can handle 500 kbps with GNU Radio without any problems. Sampling of the analog waveform occurred at the hardware's maximum performance, 64 MS/s, which was decimated in the FPGA by a factor of 256, the maximum possible in the standard GNU Radio setup. This resulted in the smallest possible baseband sampling rate of 250 kS/s, which was chosen to facilitate USB data transfer and signal processing. Similarly, interpolation on the transmitter side occurred at a factor of 512 and digital to analog conversion at a rate of 128 MS/s.

To reduce the timing recovery accuracy needed at the receivers, a root raised cosine (RRC) pulse shaping filter with 35 percent extra bandwidth was employed. Timing recovery was performed by a modified Mueller and Muller [26] algorithm with parameters as specified in Table 3.1.

Data was transferred in packets whose total length could be specified, but each of which had a 10 byte header. The first 8 bytes of the header were a constant access code to allow for packet detection at the receiver and symbol synchronization when combining packets. The remaining 2 bytes were for packet numbering. Orthogonality was obtained between the source and relay transmissions via time division.

3.1.3 Transmit Power Calibration

Control of transmit power on the USRP is coarse and no means of automatic calibration are provided. This results in varying performance from one USRP to the next. Although precise SNR knowledge is not necessary for the plotting of BER curves, the relative increase in SNR between data points should be accurate in order

to reproduce the desired graph geometry. In addition, the BER curve simulation was performed under the assumption that the average received SNRs of all links were the same, necessitating that average link performances be close to identical.

In order to manually calibrate the transmit power of the USRPs, each USRP was attached directly to a spectrum analyzer. The transmit power was then measured while the USRP sent a signal identical to that used for transmission in the relay network. Two USRPs with similar transmit powers were chosen for the source and relay nodes, the two transmitting nodes in the experiment. The quality of the receive path on the FLEX400 daughterboards also affects link performance, but it was not quantified.

3.1.4 Channel Characterization

As a model, Rayleigh fading is only appropriate when there is not a dominant line-of-sight path. Since the nodes in the experimental setup are quite close to one another and clearly have direct line-of-sight without shielding, it is quite possible that a Rician fading model is more appropriate. The Rician distribution is essentially the Rayleigh distribution with an additional term for the line-of-sight path. This new term has a deterministic magnitude and a random phase to model the direct path.

The probability density function (pdf) for the Rician distribution is [27]

$$p(r) = \frac{2(K+1)r}{\Omega} \exp\left(-K - \frac{(K+1)r^2}{\Omega}\right) I_0\left(2r\sqrt{\frac{K(K+1)}{\Omega}}\right) \quad (3.3)$$

where I_0 is the zeroth-order modified Bessel function of the first kind [28] and $\Omega = \mathbb{E}[R^2]$. The K parameter of the Rician distribution is an indication of the energy in the line-of-sight path relative to the spectral paths. The special case of $K = 0$ corresponds to the Rayleigh distribution; as K increases, so too does the strength of the line-of-sight path. A closed form expression for the probability of

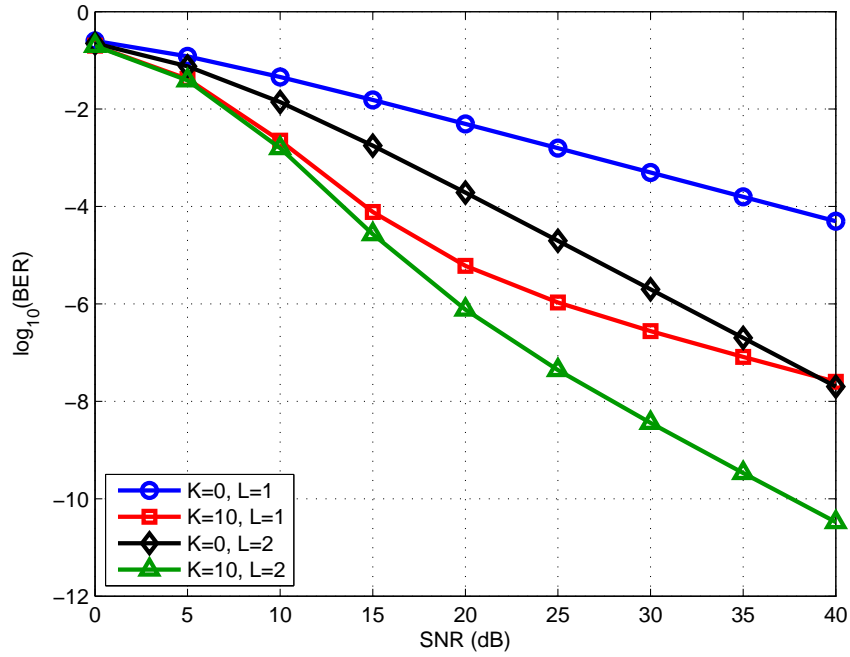


Figure 3.2: Probability of error versus SNR for DBPSK in Rayleigh ($K=0$) and Rician ($K=10$) fading

error in M-ary differential phase shift keying (M-DPSK) transmitted over the Rician fading channel with diversity is [29]

$$P_E(\text{SNR}) = \frac{\sin \frac{\pi}{M}}{2\pi} \left(\frac{L+K}{\text{SNR}} \right)^L \int_{-\pi/2}^{\pi/2} \frac{\exp \left(\frac{K(1 - \cos \frac{\pi}{M} \cos \theta)}{\frac{L+K}{\text{SNR}} + 1 - \cos \frac{\pi}{M} \cos \theta} \right)}{(1 - \cos \frac{\pi}{M} \cos \theta) \left(\frac{L+K}{\text{SNR}} + 1 - \cos \frac{\pi}{M} \cos \theta \right)^L} d\theta \quad (3.4)$$

where M is the size of the alphabet and L is the diversity order.

Figure 3.2 provides a plot of this probability of error versus SNR for $M = 2$ and different combinations of K and diversity order L . For Rayleigh fading ($K = 0$), the plots for diversity order one and two settle into their high SNR regime behavior at moderate SNR. From this plot it is easy to see the diversity gain achieved by the system operating in the Rayleigh fading environment. Although separation exists

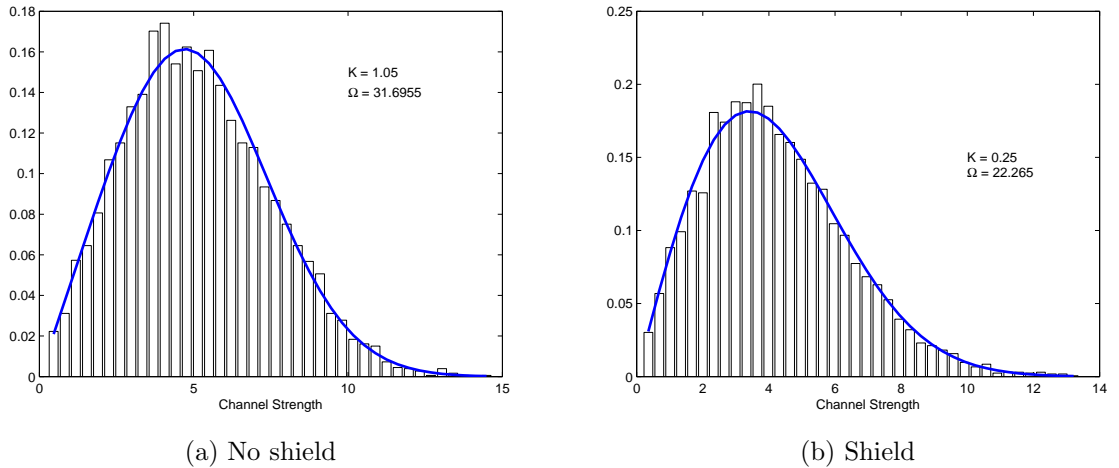


Figure 3.3: Histograms of channel strength and its approximate distribution for experimental setup (a) without shielding and (b) with shielding

between the graphs for a K value of 10 at low SNR, they do not reach their distinctive diversity order slopes until much later than the Rayleigh case. As K increases, the channel becomes closer and closer to an AWGN channel and one must look at higher and higher ranges of SNR to see the diversity gain. A strong line-of-sight path will make it difficult to observe diversity in experimentation, thus characterizing the performance of the experimental channel is of great importance.

To obtain a characterization of the channel, one node in the experimental setup was configured to transmit a pure tone at the carrier frequency. Another node recorded the magnitude of the received signal every 0.25 s. The experimental apparatus was moved in the same way as for the BER experiments as described earlier. This was done both with and without the metal shield in between the two nodes. Figures 3.3a and 3.3b plot the histograms of received signal strength for the non-shielded case and shielded case, respectively. The data was used to estimate the shape, K , and scale, Ω , parameters using a moment based estimator [27] assuming

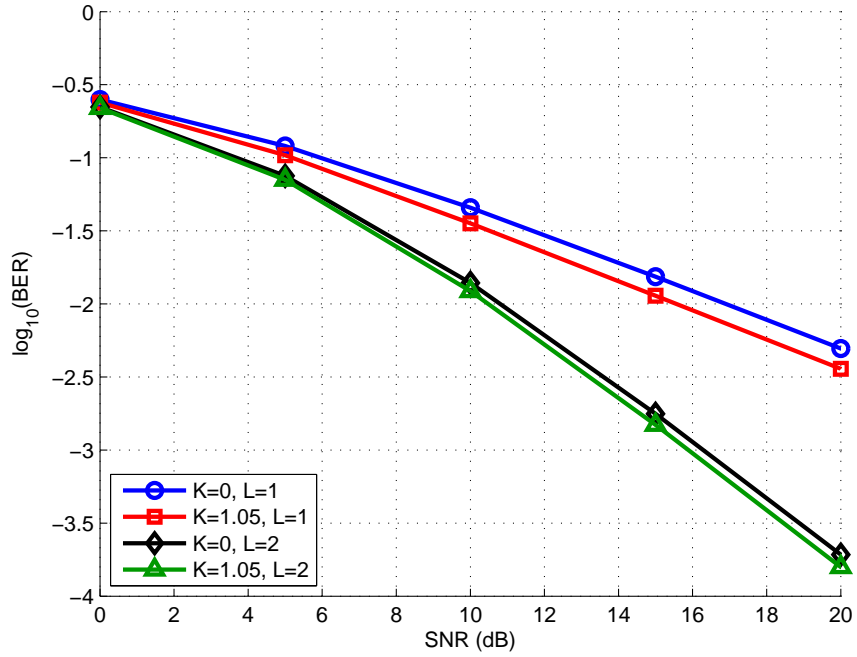


Figure 3.4: Probability of error versus SNR for DBPSK in Rayleigh ($K=0$) and Rician ($K=1.05$) fading

the data was drawn from a Rician distribution. K is the parameter of interest since it indicates how close to Rayleigh fading the channel behaves. For the non-shielded and shielded cases, the estimate of K was 1.05 and 0.25, respectively. In both cases, the fading behaves very close to Rayleigh, as can be seen by comparing the behavior of the probability of error for $K = 0$ (Rayleigh) and $K = 1.05$ and diversity orders $L = 1$ and $L = 2$ in Fig. 3.4. Theoretical analysis in the remainder of this thesis will thus assume a Rayleigh fading model.

3.2 Software Description

The system is chiefly a modification of the standard digital data transfer code that is included in the GNU Radio package. This standard GNU Radio code can

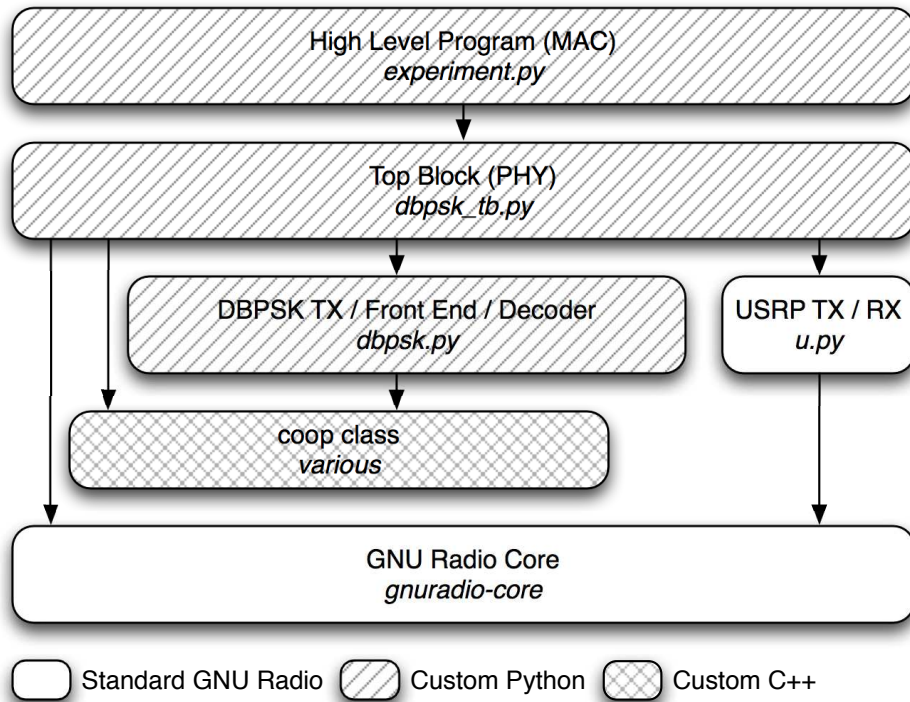


Figure 3.5: Code dependencies for BER experiment

be found in the *benchmark_tx.py* and *benchmark_rx.py* files and their dependencies. A few custom signal processing blocks were created out of necessity, which will be noted when they are described. Figure 3.5 provides a diagram of dependencies for the modified code. The highest level file *experiment.py* contains the implementation of the medium access control (MAC) layer and code controlling the experiment. It has as a dependency the physical layer implementations of the source, relay, and destination network nodes defined in the file *dbpsk_tb.py*, which in turn are dependent on the hierarchical blocks of signal processing elements defined in *dbpsk.py*.

3.2.1 Medium Access Control

Within *experiment.py*, an instantiation of the top block defined in *dbpsk_tb.py* is created. This object contains the physical layer implementations of the transmitter paths for the source and relay nodes along with physical layer receive paths for the relay and destination nodes. A diagram of the logical flow of the code in *experiment.py* is provided by Fig. 3.6. A packet composed of an access code for framing at the receiver, packet number, and randomized payload data is created and then passed to the physical layer of the source for transmission.

The program then sets a timer and polls the relay's physical layer for the packet sent from the source. If a timeout occurs, the program assumes the packet was lost and a new one is generated and sent from the source. If the packet is detected, that is, the access code is found by the relay's receive physical layer, the received packet is passed on to the relay's transmit path to be sent to the destination. Because failed packet detection is more likely to occur for poor channels, there will be a slight biasing of the experiment in favor of better channels.

Again, the program sets a timer and polls for the packet, but this time at the destination. A timeout forces a reset and packet regeneration. If two packets are received at the destination, decoded packets formed from each received packet as well as from a diversity combined version are available to the program. It compares the payloads of the decoded packets with the original random data to determine the number of bit errors occurring in each mode of transmission. These values are recorded and the process is repeated. The program iterates through a specified range of transmit powers, sending a predefined number of packets for each level.

The combining performed at the destination is equal gain combining (EGC) in which the symbols from the two paths are given equal weight in combining. It will be seen that error propagation from the relay negates any diversity gain in this

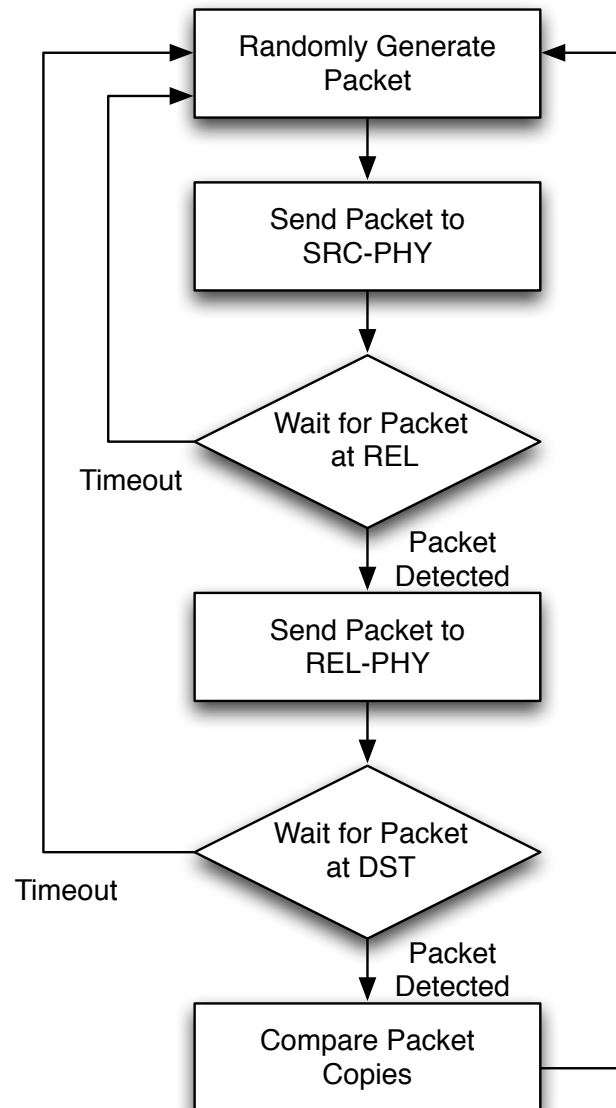


Figure 3.6: Flow diagram for BER experiment

simple DF relaying scheme. A slight modification to the *experiment.py* code will be made such that the relay only forwards packets that it decodes without error, which is determined through the use of a CRC. This is selection relaying for DF, which will also be referred to as selective DF.

3.2.2 Source Node

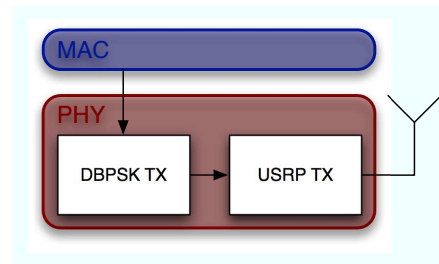
A high level block diagram of the source node is found in Fig. 3.7a. The *DBPSK TX* block is a hierarchical block defined in *dbpsk.py* and depicted in Fig. 3.8a. In it, a message source block at the head of the chain is a queue into which the binary data to be transmitted can be inserted by the MAC layer. The next block breaks the data into bit groups corresponding to the size of the symbol alphabet to be used, in this case single bits since the symbol constellation is binary. Bits are then mapped to their corresponding symbols, which are differentially encoded and transformed to a complex floating point representation. Next, the data stream is filtered by the pulse shaping filter, which in our case is a root raised cosine with a roll off factor of 0.35, as mentioned earlier. Finally, an amplifier scales the data stream allowing transmit power to be varied. The data is then passed to the USRP for transmission.

The instantiation of the USRP block sets up the USRP in a generic transmit mode. Once in the USRP, the data stream will be digitally upconverted to an IF before being converted to an analog signal. The analog signal is then mixed on the daughterboard to the desired carrier frequency and transmitted.

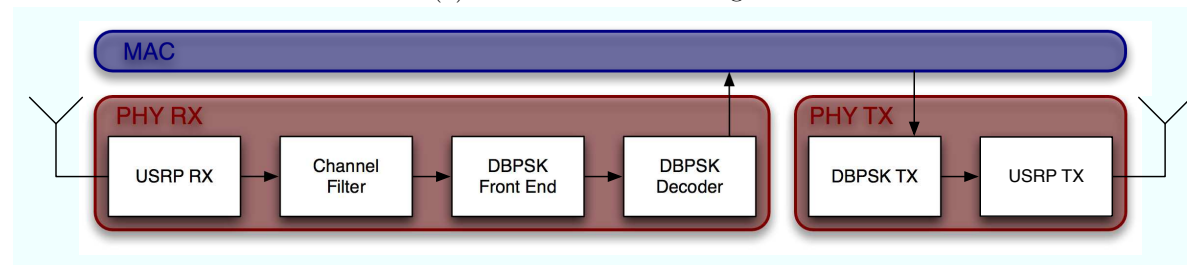
3.2.3 Relay Node

Figure 3.7b illustrates the high level block diagram for the relay node in our DF network. The transmit path physical layer for the relay node is identical to that of the source node.

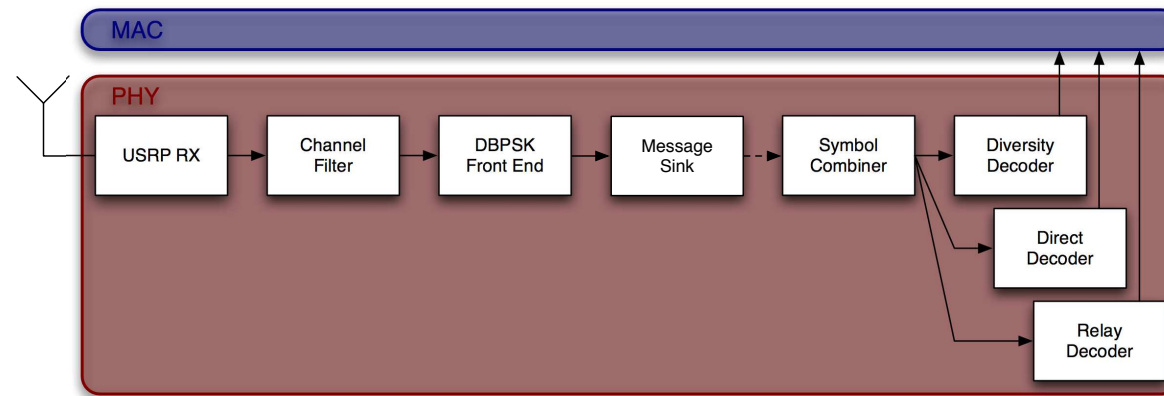
The *USRP RX* block in the receive physical layer sets up the attached USRP to



(a) Source node block diagram

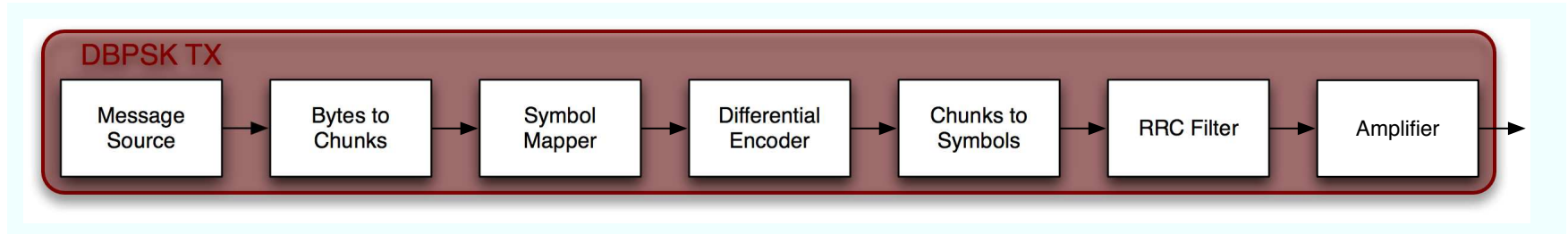


(b) Relay node block diagram

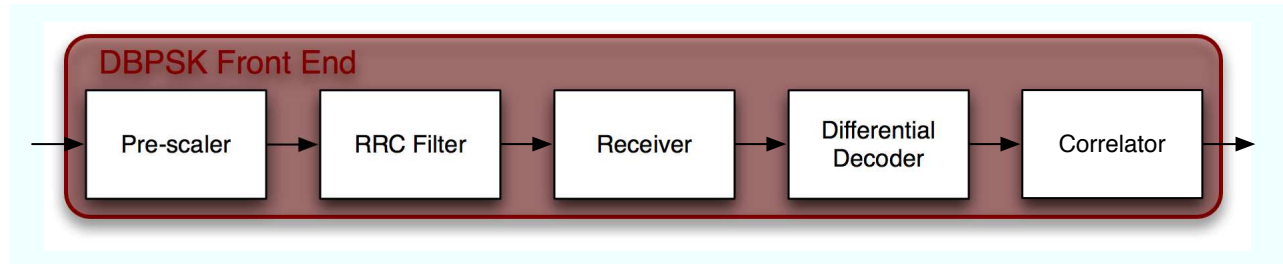


(c) Destination node block diagram

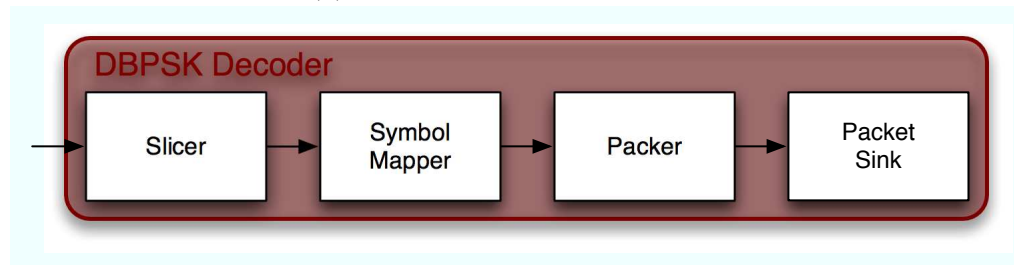
Figure 3.7: Block diagrams of decode-and-forward relay network nodes



(a) DBPSK transmitter block



(b) DBPSK receiver front end block



(c) DBPSK receiver decoding block

Figure 3.8: Hierarchical blocks for DBPSK decode-and-forward relay implementation

perform the standard receive functionality. This includes shifting the desired receive frequency to IF, sampling, and converting to baseband before sending the data to the GPP of the controlling computer via the USB link. At this point, the digital data stream is filtered by a low pass filter to attenuate signals outside the channel of interest. A diagram of the signal processing blocks incorporated in the *DBPSK Front End* block, which is defined in *dbpsk.py*, can be found in Fig. 3.8b. Within this block, the data is scaled and then filtered by the pulse shaping filter. The *receiver* block performs both timing recovery using a Mueller and Muller algorithm and carrier recovery using a Costas loop, despite the fact that differential transmission is used. Finally, the received symbols are differentially decoded and correlated with the access code to delineate the beginning of each packet. Only the symbols for a detected packet are passed by the *correlator* block. Although the framing performed by the *correlator* block could be carried out after the received symbols have been sliced, it will be necessary at the destination node that it be carried out beforehand. The *correlator* is a custom signal processing block developed for this network.

DBPSK Decoder is also defined in *dbpsk.py* and depicted in Fig. 3.8c. Within this block, the received symbols that are outputted by the *correlator* are sliced to points in the symbol constellation and mapped to the appropriate bit values. The bits are packed together to form bytes and formed into a GNU Radio message that waits in a queue to be accessed by the MAC layer.

3.2.4 Destination Node

Figure 3.7c contains the layout for the destination node. The first half of this signal processing chain is identical to that of the receive path in the relay node. The USRP is setup for reception. A low pass filter selects the desired channel of transmission out of the digital signal sent by the USRP over the USB connection.

At the output of the *DBPSK Front End* block, the *correlator* only outputs the received symbols. These symbols are grouped by packet and inserted as messages into a queue by the custom *message sink* block. The *combiner* block draws its input from this queue. Combining is why framing is performed before hard decisions are made on each symbol. In order for the *combiner* to perform pre-detection diversity combining, it must have access to the unsliced data symbols but it also must be able to align the symbols from the two received copies of a given packet.

The *combiner* block is a custom block that was created for this decode-and-forward relay network implementation. It expects to receive two copies of the same packet, one from the source and one from the relay. It waits until it has the necessary number of packets for combining before checking if the packet numbers match. If the numbers do not match, it drops the oldest packet and waits for another in order to ensure that different packets are not accidentally combined. The combiner can be instructed to perform EGC, max ratio combining (MRC), or selection combining (SC). There are three output streams from the block, one for the symbols resulting from diversity combining, one for the symbols of the direct path packet (assumed to be the first packet received), and one for the symbols of the packet received via the relay. The former two streams are used for comparative performance evaluation in the higher-level experiment program.

Each of these three data streams is connected to a *DBPSK Decoder* block which slices and finishes the decoding of the received data. The MAC layer has access to the received data as decoded by all three paths.

3.3 Summary

In this chapter the physical setup, system parameters, and software architecture for a decode-and-forward relay network implemented in SDR were described. The

physical setup consisted of an equilateral triangle that was moveable to capture multiple channel realizations while maintaining a constant average SNR between nodes. The SDR system used was a combination of GNU Radio and the USRP. A description of software for the source, relay and destination nodes in the network was also given.

CHAPTER 4

RECEIVED SYMBOL DISTRIBUTION EXPERIMENT

As will be seen in Chapter 5, obtaining an accurate BER versus SNR curve requires taking large amounts of data at numerous SNR values. Furthermore, as SNR increases, the expected BER will decrease, necessitating evermore data to obtain an accurate BER estimate. This chapter explores looking at a histogram of received symbols for a fixed transmit power and internode distance to detect the presence of diversity. Although this simpler method cannot conclusively prove the presence of a diversity gain, it can hint at it. Experimental use of this metric in our setup will show that diversity is likely occurring for our simple DF relaying scheme and selective DF scheme.

4.1 Theoretical Basis

This section will provide a theoretical basis for looking at the distribution of received symbols as an indicator of possible diversity in our simple DF scheme.

4.1.1 Direct Transmission

For simplifying implementation, all experiments were performed with differential encoding, where the information to be sent is carried in the change of phase between the transmitted symbols. The following analysis is performed using a discrete time

channel model assumed to have the form

$$r = hs + w \quad (4.1)$$

where s is the transmitted symbol drawn from a binary alphabet $\{-1, +1\}$, h is the channel gain used to model the multipath fading, which is a zero-mean, complex Gaussian random variable in the Rayleigh fading case. The term w is the thermal noise at the receiver, modeled as a complex, zero-mean, circularly symmetric Gaussian random variable with two-sided noise variance $N_0/2$. The received symbol is r . Since the information in differential encoding is carried on the change of phase between successive transmitted symbols, the information symbol sent at time instance i , x_i , can be recovered from the transmitted symbols s_i and s_{i-1} by the relationship $x_i = s_i s_{i-1}^*$. The receiver will apply the following rule to form a statistic y_i for estimating the data symbol x_i

$$y_i = r_i r_{i-1}^* \quad (4.2)$$

$$= (hs_i + w_i)(hs_{i-1} + w_{i-1})^* \quad (4.3)$$

$$= |h|^2 x_i + hs_i w_{i-1}^* + w_i s_{i-1}^* h^* + w_i w_{i-1}^*. \quad (4.4)$$

The slow fading assumption also allows us to assume that h remains constant between successive symbols. As is commonly done to make performance analysis more tractable [30], the last term in Eq. 4.4 is ignored since it is the multiplication of two independent noise terms, and the cross terms are simplified as follows. The transmitted symbols have $|s_i| = 1$ and thus are purely phase terms corresponding to a rotation. Since the w_i are circularly symmetric, this rotation will have no effect on the variance of the cross terms, and the s_i can be ignored. For a given realization of the channel coefficient h , the cross terms will remain Gaussian random variables

with variance

$$\text{Var}[hw_i|h] = \mathbb{E}[(hw_i)(hw_i)^*|h] \quad (4.5)$$

$$= \mathbb{E}[hw_iw_i^*h^*|h] \quad (4.6)$$

$$= |h|^2\mathbb{E}[w_iw_i^*|h] \quad (4.7)$$

$$= |h|^2N_0. \quad (4.8)$$

Since the w_i are independent and identically-distributed (i.i.d.), their sum will be another zero-mean, Gaussian random variable with variance equal to the sum of the two individual variances, or $2|h|^2N_0$. If $h \sim \mathcal{CN}(0,1)$, then the magnitude $|h|$ is Rayleigh distributed and $|h|^2$ is Chi-square distributed with two degrees of freedom, which is the same as an exponential distribution with parameter $\lambda = 1$.

Because the alphabet is binary and purely real, the receiver need only be concerned with the real component of the received symbol. The effects of differential encoding can be incorporated into a modified channel model that, rather than relating the transmitted and received symbols, relates the data symbol and the destination's estimate of the data symbol by

$$y = \gamma x + n \quad (4.9)$$

where $\gamma = |h|^2 \sim \mathcal{E}\mathcal{X}\mathcal{P}(1)$ and $n \sim \mathcal{N}(0, \gamma N_0)$. The noise variance is the one dimensional variance $N_0/2$ from Eq. 4.1, since the alphabet is purely real, scaled by 2γ due to the differential encoding. From this point on the channel model of Eq. 4.9 will be used for analysis and x will be referred to as the transmitted symbol, y as the received symbol. Conditioning on the channel gain and the transmitted symbol, the received symbol will also be normally distributed with $y \sim \mathcal{N}(\gamma x, \gamma N_0)$. Performing minimum distance detection, the receiver uses the sign of the received symbol y to estimate the transmitted symbol x . A detection error will occur whenever the received symbol y has the opposite sign of x . Due to the symmetry of the problem,

we can assume without loss of generality that the transmitted symbol was $x = +1$. The term γ will clearly have an impact on the probability of decoding error by shifting the mean of the distribution of the received symbol. A small value will increase the likelihood of error, and a large value will decrease the likelihood of error. To get an idea of what the distribution of received symbols will look like for direct transmission over the slow fading channel, we need to average over the range of channel gains

$$p(y|x = 1) = \int_0^\infty p(y, \gamma|x = 1)d\gamma \quad (4.10)$$

$$= \int_0^\infty p(y|\gamma, x = 1)p(\gamma)d\gamma \quad (4.11)$$

$$= \int_0^\infty \frac{1}{\sigma\sqrt{2\pi}} \exp\left(-\frac{(y - \gamma)^2}{2\sigma^2}\right) \exp(-\gamma)d\gamma \quad (4.12)$$

where $\sigma^2 = \gamma N_0$. This integral was evaluated numerically and is plotted in Fig. 4.2. It will be compared with the received symbol distribution for the simple DF relay network.

4.1.2 Simple Decode-and-Forward Relaying

Figure 4.1 shows the model for our simple DF relay network. The derivation here has many similarities with the work done in [31], though the end goal is different. Leaning on the analysis provided in the previous section, for the DF relay network let $x_S, x_R \in \{-1, +1\}$ be the transmitted symbols from the source and relay. The channel gains for each link are $\gamma_{SD}, \gamma_{SR}, \gamma_{RD} \sim \mathcal{E}\mathcal{X}\mathcal{P}(1)$ for the S-D, S-R, and R-D links, respectively. Transmissions of the source and relay are assumed to occur in non-interfering, orthogonal channels obtained through either time or frequency division multiplexing. Thermal noise terms are $n_R, n_{D_1}, n_{D_2} \sim \mathcal{N}(0, \gamma N_0)$ at the relay, the destination while receiving the source's transmission, and the destination while receiving the relay's transmission, respectively. The received symbols have the

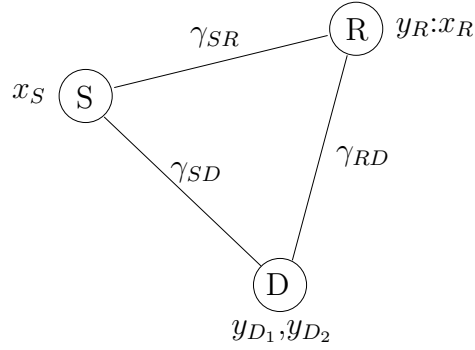


Figure 4.1: Probabilistic model for three node decode-and-forward relay network

following relationships

$$y_R = \gamma_{SR}x_S + n_R \quad (4.13)$$

$$y_{D_1} = \gamma_{SD}x_S + n_{D_1} \quad (4.14)$$

$$y_{D_2} = \gamma_{RD}x_R + n_{D_2} \quad (4.15)$$

where y_R, y_{D_1} are the reception of the source's transmitted symbol at the relay and destination, and y_{D_2} is the reception of the relay's transmitted symbol at the destination. Each of these three individual channels is identical to the direct transmission channel derived in the previous section.

Because the relay employs DF relaying, it will make a hard decision about what symbol was transmitted by the source and transmit this estimate on to the destination. Error propagation occurs when the relay fails to correctly estimate the source's symbol, and thus forwards the wrong symbol to the destination. The destination uses a combined version of its two received symbols y_{D_1}, y_{D_2} to estimate the message sent by the source. An EGC diversity combiner is simple to implement. Unlike an MRC which needs channel knowledge to weight the received symbols, EGC simply gives equal weight to both. The statistic formed by the EGC at the destination in

the experimental setup to estimate x_S is

$$y = y_{D_1} + y_{D_2}. \quad (4.16)$$

We want to compare the distribution of received symbols for the diversity case, which corresponds to using our new statistic y , with that of the direct transmission case, which corresponds to solely using y_{D_1} . Assuming again that $x_S = +1$, the direct transmission will have a distribution defined by Eq. 4.12. We need to find the distribution for the new statistic y . If all three channel gains are known, we can write the conditional probabilities of y_R and y_{D_1} as

$$p(y_R|\gamma_{SR}, x_s = 1) \sim \mathcal{N}(\gamma_{SR}, \gamma_{SR}N_0) \quad (4.17)$$

$$p(y_{D_1}|\gamma_{SD}, x_s = 1) \sim \mathcal{N}(\gamma_{SD}, \gamma_{SD}N_0) \quad (4.18)$$

for reception of the source's symbol. The distribution for y_{D_2} is more involved, since it is possible for x_R to differ from x_S . For a given S-R channel realization, the probability that the relay makes an error in detection in DBPSK is known to be [30]

$$P_E = Q(\sqrt{\gamma_{SR}SNR}) \quad (4.19)$$

$$= Q\left(\sqrt{\frac{\gamma_{SR}}{N_0}}\right) \quad (4.20)$$

where $Q(\cdot)$ is the Q-function

$$Q(z) = \frac{1}{\sqrt{2\pi}} \int_z^\infty \exp\left(-\frac{t^2}{2}\right) dt \quad (4.21)$$

and Eq. 4.20 is with our parameters. We can write the distribution for x_R as

$$p(x_R|\gamma_{SR}, x_S = 1) = \begin{cases} 1 - P_E & \text{for } x_R = 1 \\ P_E & \text{for } x_R = -1 \end{cases} \quad (4.22)$$

Conditioning on x_R and γ_{RD} , y_{D_2} will be

$$y_{D_2} \sim \begin{cases} \mathcal{N}(\gamma_{RD}, \gamma_{RD}N_0) & \text{if } x_R = 1 \\ \mathcal{N}(-\gamma_{RD}, \gamma_{RD}N_0) & \text{if } x_R = -1 \end{cases} \quad (4.23)$$

In either case, y_{D_2} conditioned on the R-D channel ends up being a Gaussian random variable. Since y_{D_1} is independent and also a Gaussian random variable assuming γ_{SR} is known, the combination $y_{D_1} + y_{D_2}$ will be a Gaussian random variable with a mean and variance equal to the sum of the two components' means and variances. Hence we have

$$y \sim \begin{cases} \mathcal{N}(\gamma_{SD} + \gamma_{RD}, (\gamma_{SD} + \gamma_{RD})N_0) & \text{if } x_R = 1 \\ \mathcal{N}(\gamma_{SD} - \gamma_{RD}, (\gamma_{SD} + \gamma_{RD})N_0) & \text{if } x_R = -1 \end{cases} \quad (4.24)$$

Since we know the probability that x_R takes on one of its two possible values, we can finally write

$$p(y|\gamma_{SD}, \gamma_{SR}, \gamma_{RD}, x_S = 1) = (1 - P_E) \frac{1}{\sigma_y \sqrt{2\pi}} \exp\left(-\frac{(y - \mu_1)^2}{2\sigma_y^2}\right) + P_E \frac{1}{\sigma_y \sqrt{2\pi}} \exp\left(-\frac{(y - \mu_2)^2}{2\sigma_y^2}\right) \quad (4.25)$$

where

$$\mu_1 = \gamma_{SD} + \gamma_{RD} \quad (4.26)$$

$$\mu_2 = \gamma_{SD} - \gamma_{RD} \quad (4.27)$$

$$\sigma_y^2 = (\gamma_{SD} + \gamma_{RD})N_0 \quad (4.28)$$

$$P_E = Q\left(\sqrt{\frac{\gamma_{SR}}{N_0}}\right). \quad (4.29)$$

Finally, we average over the channel gains by integrating

$$p(y|x_S = 1) = \iiint p(y|\gamma_{SD}, \gamma_{SR}, \gamma_{RD}, x_S = 1) p(\gamma_{SD}) p(\gamma_{SR}) p(\gamma_{RD}) d\gamma_{SD} d\gamma_{SR} d\gamma_{RD} \quad (4.30)$$

which is plotted along with the direct transmission case in Fig. 4.2. Additionally, the received symbol distribution for transmit diversity is plotted as well. Assuming that the relay always correctly decodes the source's transmission will reduce the simple DF scheme to a transmit diversity scheme; thus, transmit diversity provides an upper

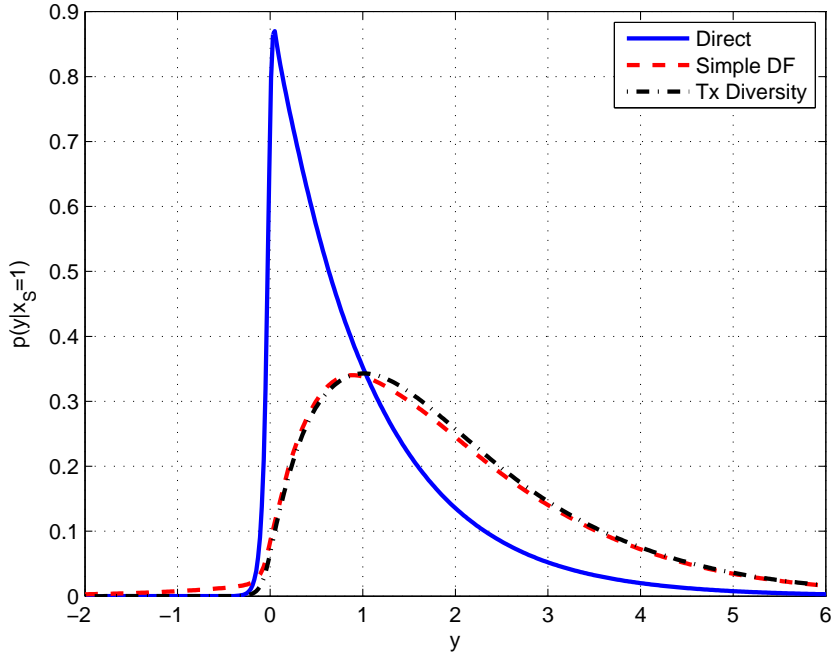


Figure 4.2: Probability distributions of received symbols for direct transmission, simple DF, and transmit diversity

bound on the performance of our simple DF scheme. Obtaining the distribution for transmit diversity from Eq. 4.30 simply requires assuming that $P_E = 0$ in Eq. 4.25 and ignoring the integral over γ_{SR} . The parameter N_0 was chosen to give an average received SNR of 10 dB for each link.

4.1.3 Direct and Diversity Comparison

The direct and simple DF densities plotted in Fig. 4.2 have distinctive shapes. What is the relationship between this difference in shape and the presence of diversity? In [32], diversity is quantified using the behavior of the instantaneous SNR distribution around the origin. In fact, the authors show that different distributions for the instantaneous SNR can be thought of as providing different amounts

of diversity. Instantaneous SNR is a combination of average SNR and the channel random variable. In the diversity path, it is dependent on a combination of the channel random variables from both paths. Transmissions that occur when the instantaneous SNR is very small produce the most errors, making the instantaneous SNR's behavior around the origin of greatest importance. The authors show that the diversity order of a system can be obtained based on the smoothness of the density function around the origin, or equivalently, the decay order of the related moment generating function.

It is similar here with our distinctive histograms. The different behavior of the instantaneous SNR distributions for the direct and diversity paths results in distinctive received symbol distributions. For direct transmission, the received distribution is the averaging of Gaussian distributions centered at the instantaneous SNR, which is distributed according to the Chi-square distribution with two degrees of freedom, equivalent to an exponential distribution. Simplifying by assuming the relay makes no errors, the received symbol distribution for transmit diversity is the averaging of Gaussian distributions at instantaneous SNRs that are distributed with a Chi-square distribution with four degrees of freedom. The additional degrees of freedom for this path come from the combining of the two channel gains. The difference between the Chi-square distributions of two and four degrees is distinctive, especially at the origin.

In our case of simple DF relaying, the effective SNR distribution is slightly more complicated, but the same idea holds. There must be a change in the instantaneous SNR distribution, specifically around the origin, for diversity to be present. The overall behavior of the simple DF and transmit diversity distributions is very similar. Since transmit diversity is known to provide full diversity, this is encouraging.

Another difference in the behavior of the direct and simple DF distributions

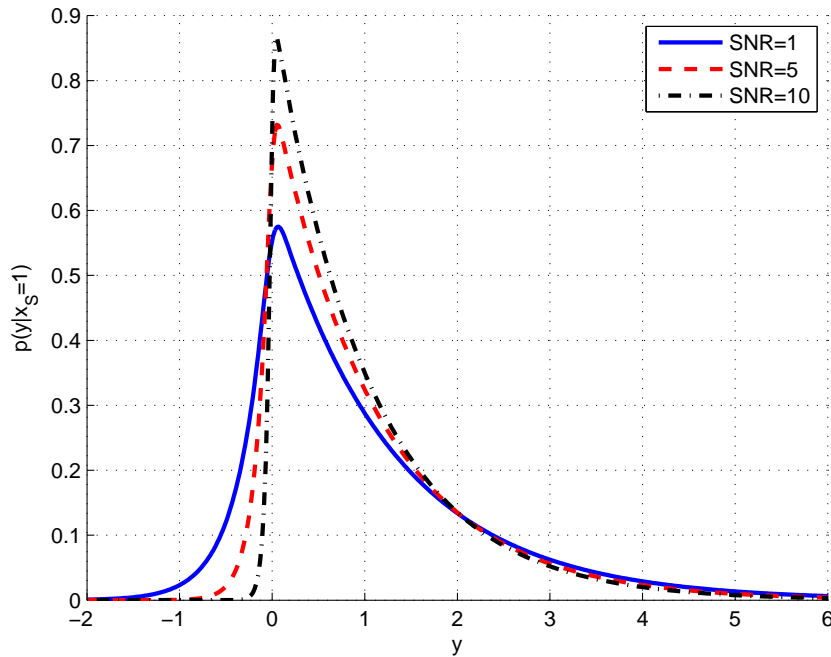


Figure 4.3: Probability distribution of received symbols for direct transmission for different values of average SNR

is that simple DF uses twice as much power as direct transmission. In the relay scheme, the source symbol is transmitted with both the power of the source and relay (albeit with the possibility of errors being introduced at the relay). Would doubling the power the source uses to transmit lead to the same distributions as the diversity schemes? Figure 4.3 shows the distribution of received symbols for direct transmission at various average SNR values. Although performance of the scheme improves with more power, there is no fundamental change in the shape of the distribution resembling the distribution of symbols for diversity seen in Fig. 4.2. The change in the received symbol distribution allows us to observe a modification in the instantaneous SNR distribution.

In looking at Fig. 4.2, it is important to keep in mind that a change in the

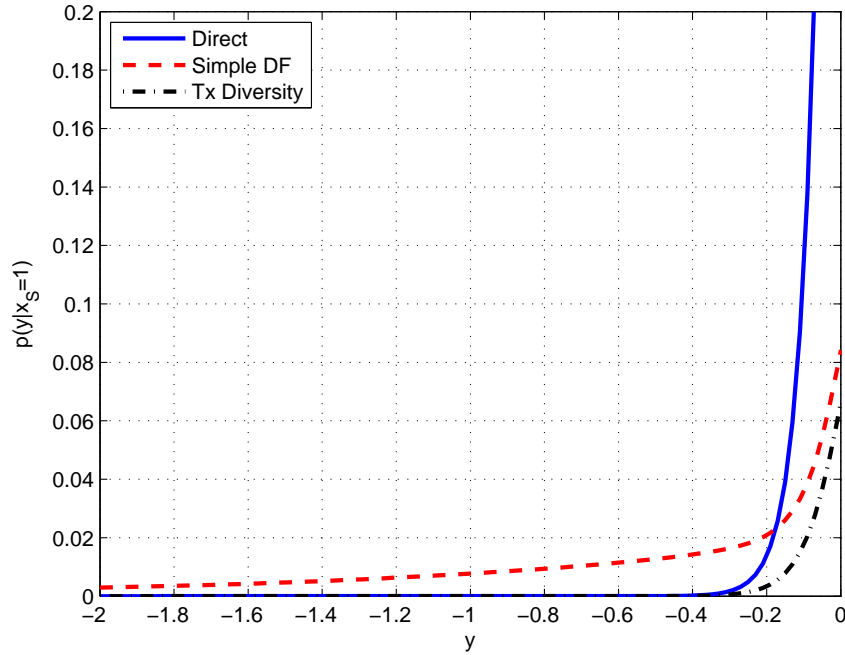


Figure 4.4: Probability distributions of received symbols for direct, simple DF, and transmit diversity left of the origin

received symbol distribution, or equivalently the instantaneous SNR distribution, does not in itself prove that a diversity gain has been created. The distributions are conditioned on the fact that $x_S = 1$; as such, all of the probability mass to the left of zero is the likelihood that the destination will make an error when deciding about the symbol sent by the source. Figure 4.4 magnifies the behavior of the three distributions to the left of the origin. Clearly, transmit diversity has less mass than the other two schemes and will have better performance. The simple DF graph resembles the transmit diversity graph here as well, but it has more probability mass due to error propagation. Between direct and simple DF transmission it is not obvious which scheme has less mass and better performance.

We can integrate our density functions to get a value for the probability of error

at the destination for our direct and simple DF transmission methods

$$P_{y_{D_1}} = \int_{-\infty}^0 p(y_{D_1}|x_S = 1)dy_{D_1} \quad (4.31)$$

$$P_y = \int_{-\infty}^0 p(y|x_S = 1)dy. \quad (4.32)$$

For our chosen value of N_0 we obtain

$$\log_{10}(P_{y_{D_1}}) = -1.39 \quad (4.33)$$

$$\log_{10}(P_y) = -1.59. \quad (4.34)$$

The DF relay scheme theoretically outperforms the direct transmission scenario for this average SNR. The question arises if the better performance of the relay scheme is truly a result of a diversity gain or if it only comes from having more power in the system. This is something that cannot be decided without analysis for different average SNR values, which essentially requires plotting the BER versus SNR curve.

We can conclude that the unique shape of the received symbol distribution for the diversity case can be compared with the distribution in the direct scenario to tell whether or not the instantaneous SNR distribution has been altered. This modification of the instantaneous SNR distribution is essential for producing diversity, but a change does not in itself prove the presence of diversity. To do this, analysis of the received symbol distribution around the origin is necessary. This is similar to obtaining BER versus SNR curves. However, looking at the received symbol distribution is much simpler than obtaining BER curves and can at the very least show if a diversity gain is possible.

As a further confirmation of the expected received symbol distribution at the destination, the DBPSK simple DF relay network was simulated with the same parameters used in the theoretical analysis made above. Figure 4.5 shows the result. These histograms match what would be expected if our densities in Fig. 4.2 were not conditioned on the transmitted symbol.

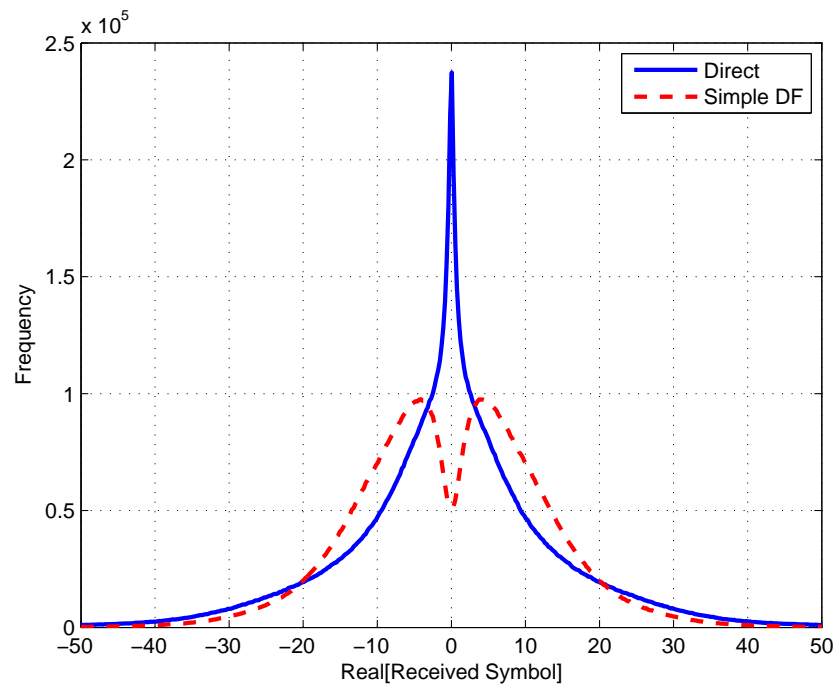


Figure 4.5: Histograms of received symbols for simulated DBPSK direct and simple DF relay transmission

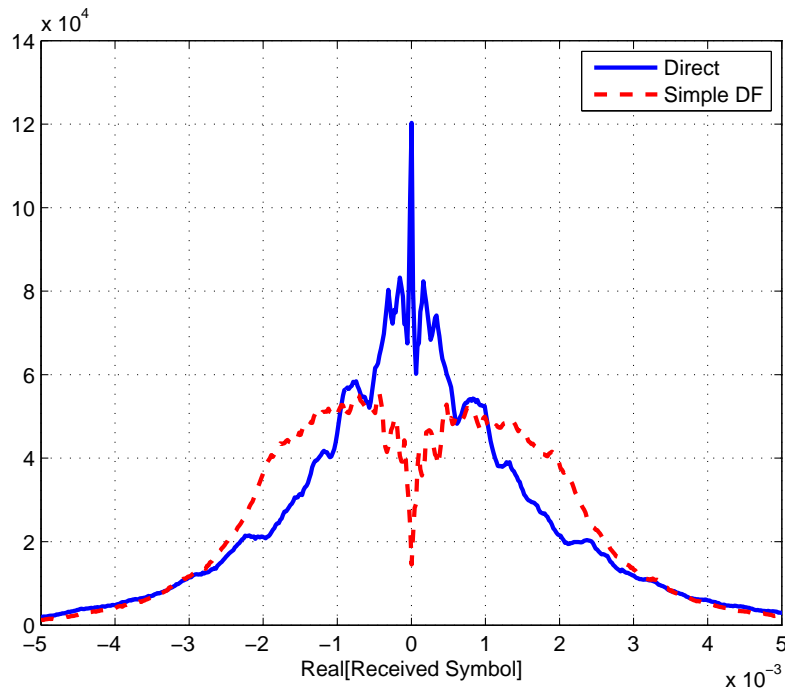


Figure 4.6: Histograms of received symbols for experimental DBPSK direct and simple DF relay transmission

4.2 Experimental Results

The simple DF experimental system described in Chapter 3 was modified to save all received symbols. All nodes were fixed approximately 2.6 m away from one another. To obtain different channel realizations, the setup was moved around the hallway while sending one packet of 500 bytes at a time. Figure 4.6 shows the histogram of received symbols for both the direct and diversity transmission cases for 5000 channel realizations.

There is a clear distinction between the two histograms in the experimental data that mirrors that observed in the analytical work, Fig. 4.2, and simulation, Fig. 4.5. The diversity scheme has two distinctive lobes, while the direct scheme

has a single peak centered at zero. These shapes match those of the simulated histograms and analytically determined distributions if the analytical distributions were not conditioned on the transmitted symbol. Fewer symbols for the diversity scheme are close to zero as compared with the direct scenario. This reduction in the number of symbols about the origin should translate into better performance for the diversity scheme. Because the histograms behave similarly to the distributions of the previous section, we can conclude that our experimental setup is indeed showing some modification to the instantaneous SNR distribution and diversity could be occurring. However, differing histograms do not guarantee the presence of diversity.

4.3 Summary

It has been shown that the distribution of received symbols is distinctive for the DF relay network as compared with direct transmission. This distinction was used to validate a change in the instantaneous SNR distribution in the experimental setup. The data taken experimentally matches the theoretical prediction and simulation, but does not in itself prove that the cooperative scheme actually provides diversity, only that a reshaping of the instantaneous SNR distribution is present. The next chapter looks at experimental BER values to determine whether the experimental network actually enjoys a diversity gain.

CHAPTER 5

BER CURVE EXPERIMENT

In this chapter, the results for the experimental determination of BER versus SNR curves for the DF network are presented and analyzed. A short explanation is given of what signs are expected if diversity is present, followed by some considerations for different DF schemes. The experimental system is simulated to determine the expected results for the various DF schemes. Experimental BER plots with EGC at the destination for both simple DF and selective DF relaying schemes are provided. The results for the combined paths in these systems indicate diversity is present in the latter, but not the former.

5.1 Theoretical Considerations

As explained in Chapter 2, the most common way of describing the gain provided by a system with diversity is to characterize the behavior of the BER at high SNR. In a slow fading environment, when plotted on a log-log scale versus SNR, the BER curve for a DBPSK system without diversity will decay one order of magnitude for every 10 dB increase in the average SNR. A system providing diversity will display a steeper negative slope. For full diversity, the negative slope of this line will be equal to the number of independently faded copies of the message that are available at the destination.

As of yet, no simple DF scheme has been proven to guarantee full diversity due to the error propagation that results from hard decisions made on received symbols at the relay. Maximum likelihood (ML) decoding [33] in DF schemes includes a nonlinear function that effectively limits the contribution of the sufficient statistic generated from the relay path. Intuitively, this clipping reduces the impact of error propagation from the relay. Without it, a combination of a weak S-R channel, which results in many decoding errors at the relay, and a strong R-D channel, which will lead the relay path to dominate the direct path, can severely impact performance. The use of a piece-wise linear function to approximate the nonlinear ML limiting function can be used as a simplification [34]; for both cases, the level at which the statistic is clipped is related to the probability of decoding error at the relay. Another approach is to use $\min\{\gamma_{SR}, \gamma_{RD}\}$ to weight the relay path with the weakest of the two component channels [31]. Selection relaying is a modification to DF in which only correctly decoded messages at the relay are forwarded on to the destination. The integrity of a message at the relay can be checked via a CRC, which will not catch all errors, but does have low complexity.

5.2 Simulation of BER for DBPSK System

This section provides BER simulation results for a model of the implemented DF relay network. The model used for simulation has identical parameters to those described in Chapter 4. Randomly generated data is encoded differentially with a binary alphabet. The relay fully decodes each message it receives before re-encoding and forwarding it on to the destination. EGC is used at the destination for diversity combining. A range of average SNR values are considered. In the previous chapter, we saw a shift in the received symbol distribution accompanied our diversity schemes in both theory and practice. Now we wish to ascertain whether this shift led to a

diversity gain.

Since the BER is decreasing with increasing SNR, larger values of SNR will require more simulation to acquire estimates of the BER with similar accuracy. The estimate of the BER is formed at a given SNR by

$$\widehat{\text{BER}} = \frac{k}{n} \quad (5.1)$$

where k is the observed number of errors in n bits of data sent with a given average SNR. Since k is binomially distributed, it is easy to show this estimate is unbiased. It is desirable that the data points all have similar accuracy, which means the number of bits n at each SNR must increase as SNR increases. To do this we can fix the ratio of the standard deviation of the estimate to the mean of the estimate

$$\frac{\sqrt{\text{Var}\{\widehat{\text{BER}}\}}}{\mathbb{E}\{\widehat{\text{BER}}\}} = \frac{\sqrt{\frac{p}{n}}}{p} \quad (5.2)$$

$$= \frac{1}{\sqrt{np}}. \quad (5.3)$$

For every order of magnitude decrease in the BER, n will need to be increased by a factor of 10. In the best case scenario of full diversity, we expect to see the BER decrease at a rate of two orders of magnitude per decade increase in average SNR, so we must increase the number of packets sent by a factor of 100 for every 10 dB increase in SNR. The exact number of bits to average over requires some prior knowledge of the expected BER for a given SNR. Furthermore, since errors within a packet will be correlated, we will use the number of packets instead of the total number of bits to gauge the accuracy of the estimate.

Figure 5.1 shows the results of simulating BER for direct, transmit diversity, simple DF, and selective DF transmission. Data was sent in packets of 100 bytes (800 bits or symbols). The direct transmission curve decays with approximately the expected rate of one order of magnitude per decade. Transmit diversity provides an

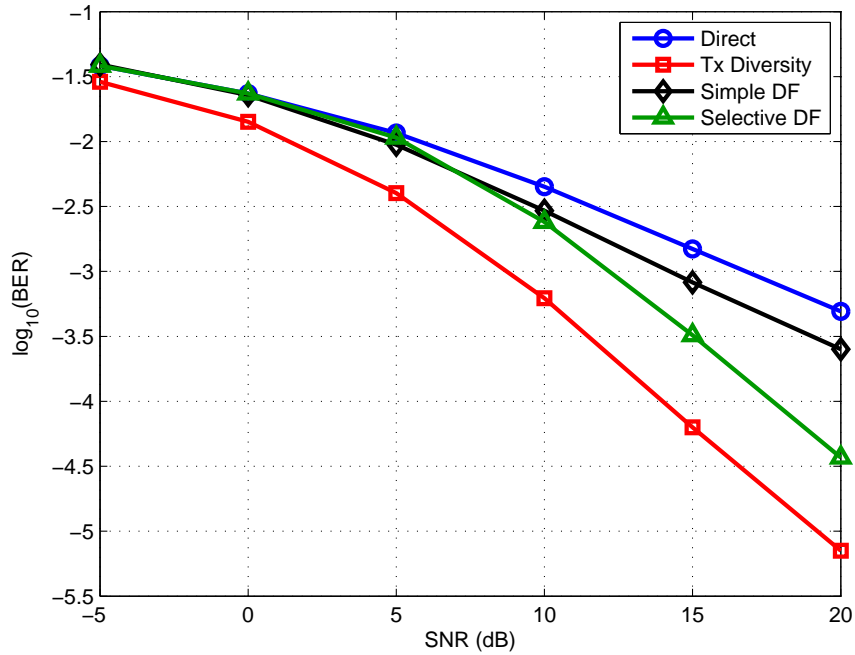


Figure 5.1: Simulation of BER versus SNR for three node decode-and-forward relay network for various transmission schemes

upper bound on decode-and-forward performance since it can be viewed as a decode-and-forward scheme that has a perfect S-R channel. It displays approximately full diversity by decaying roughly two orders of magnitude per decade.

The simple DF scheme that allows errors to propagate from the relay decays at about the same rate as direct transmission, indicating that it does not provide diversity. Here, the error propagation from the relay is eliminating any benefits obtained through having multiple copies of the transmission. This confirms the need to limit the effect of errors forwarded from the relay that was indicated by the form of the ML decoder. The separation between the two graphs comes from the additional power present in the relay system. Despite the shift in received symbol distribution seen in the previous chapter, the simple DF scheme is not able to provide

a diversity gain. Effectively, the overall density function for the instantaneous SNR is changing, but the behavior around the origin is not doing so in a way that increases the diversity order of the system.

Selective DF requires higher SNR than transmit diversity to provide noticeable benefits. At low SNR, the error rate at the relay is high, causing most packets to contain errors and not be forwarded on to the destination. Performance for selection relaying is thus similar to that of direct transmission in this regime. As the SNR increases, however, more and more packets are decoded by the relay without error and forwarded, providing greater diversity gain. The diversity order of the scheme appears to increase with increasing SNR, which stems from the increasing percentage of transmissions where the destination has two copies of the message for decoding.

5.3 Simple Decode-and-Forward Experimental Results

Experimental BER curves are provided in this section for the described relay network that uses simple DF at the relay. Data was transmitted in packets of size 500 bytes (4000 bits or symbols) for three different transmit power values. The experimental setup was moved as described in Chapter 3 to ensure packets experienced independent channel realizations. To plot the BER versus SNR curves, the squares of the software amplifier gains were used. These gains were chosen such that there would be a constant spacing between the points of 10 dB. The magnitude of the output analog signal scales linearly with these gains. Though the values used to plot for a given data point may not correspond to an accurate average received SNR in an absolute sense, they are correctly spaced relative to one another. This was verified in the transmit power calibration. Transmit amplitudes of 31.6, 100, and 316 were used with 10^2 , 10^3 , and 10^4 packets sent over each, respectively.

BER curves for the three individual links are plotted in Fig. 5.2. All three curves

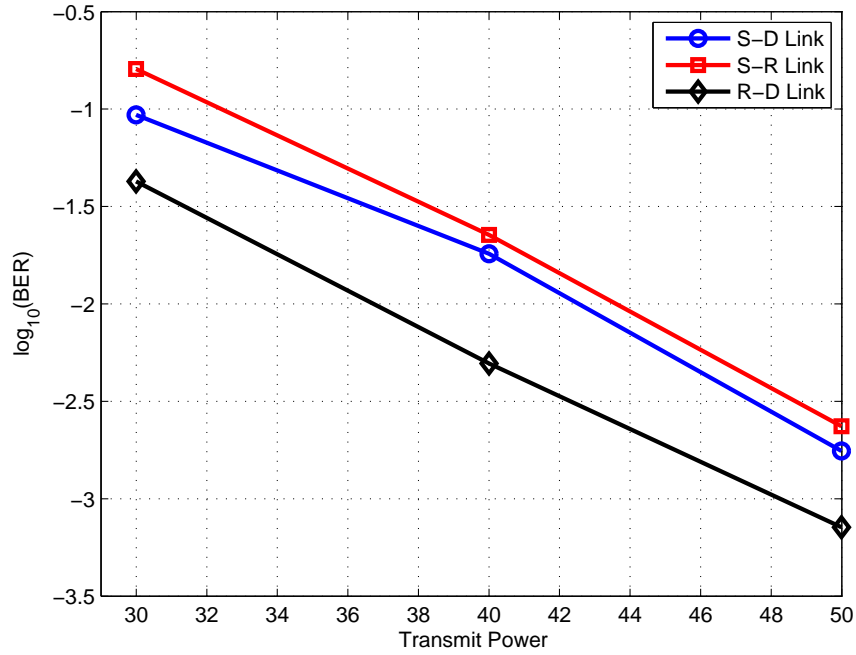


Figure 5.2: BER versus transmit power for three individual links in simple DF relay network

decrease at approximately the expected rate of one order of magnitude per decade of transmit power. The decay of the graphs further confirms that experimentation was done in a near Rayleigh environment. The R-D link has considerably better performance than both the S-D and S-R links. The S-R link is the worst, performing slightly worse than the S-D. This is the critical link that controls the effectiveness of DF.

Figure 5.3 plots the BER for both direct transmission and simple DF diversity combining. The two lines are very close to one another, decaying with approximately the same slope of one order of magnitude per decade of SNR. Clearly, the presence of diversity cannot be inferred from this graph. Furthermore, the separation between the curves expected from a larger total power in the diversity system is also missing.

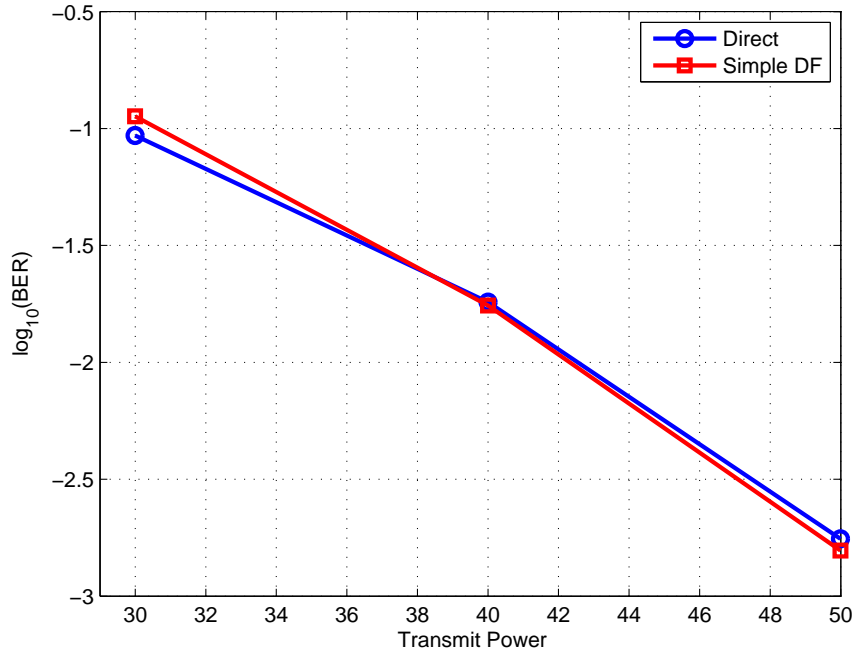


Figure 5.3: BER versus transmit power for direct and diversity paths in simple DF relay network

From this data, the direct link is performing better than the diversity link, since it has approximately the same BER curve but uses half as much power. Without a means of combatting error propagation at the relay, this scheme fails to provide diversity. This data confirms what was seen in the simulation section for the simple DF scheme and further indicates that the received symbol distribution shift is not a guarantee of diversity benefits.

5.4 Selective Decode-and-Forward Results

In the previous section, the use of simple DF relaying and EGC at the destination failed to provide diversity gain in our experimental system. A lack of compensation for the hard decisions made at the relay created a situation where forwarded errors

could dominate at the destination, canceling any diversity gains. The experimental setup was modified so that the relay would only forward packets that were received without errors, reducing error propagation. To detect errors, a 32 bit CRC was appended to each packet and checked at the relay. Although a CRC could not guarantee all errors were detected, it did greatly reduce the number of errors forwarded on to the destination. If the destination failed to receive a packet from the relay, it relied solely on the source's packet for the diversity path.

The experiment was conducted identically to that of the previous section except that the transmit powers of 31.6, 100, and 316 were given 10^3 , 10^4 , and 10^5 channel realizations, respectively. This is not the factor of 100 increase per decade of SNR required to have BER estimates of similar accuracy. Relatively fewer channels were used at higher SNRs in the interest of making the time of data collection more reasonable. It took approximately 10 hours to collect the data for this experiment.

Figure 5.4 shows the performance results of the three individual links. Of the three, the S-R link has the worst performance, with the S-D and R-D links performing nearly identical. Again, the slopes of the graphs are consistent with what would be expected from DBPSK operating in a Rayleigh fading environment.

Experimental BER curves for the direct path and diversity path are given in Fig. 5.5. The direct path has the expected slope for a scheme without diversity, but here the diversity path employing selective DF is indeed providing diversity. The slope is considerably steeper than that of the direct path, indicating a larger gain in performance for a given increase in SNR when compared with direct transmission. The scheme does not appear to provide the full diversity order of two, as was also the case in the simulation results, but the reduction in error propagation has enabled the scheme to provide diversity.

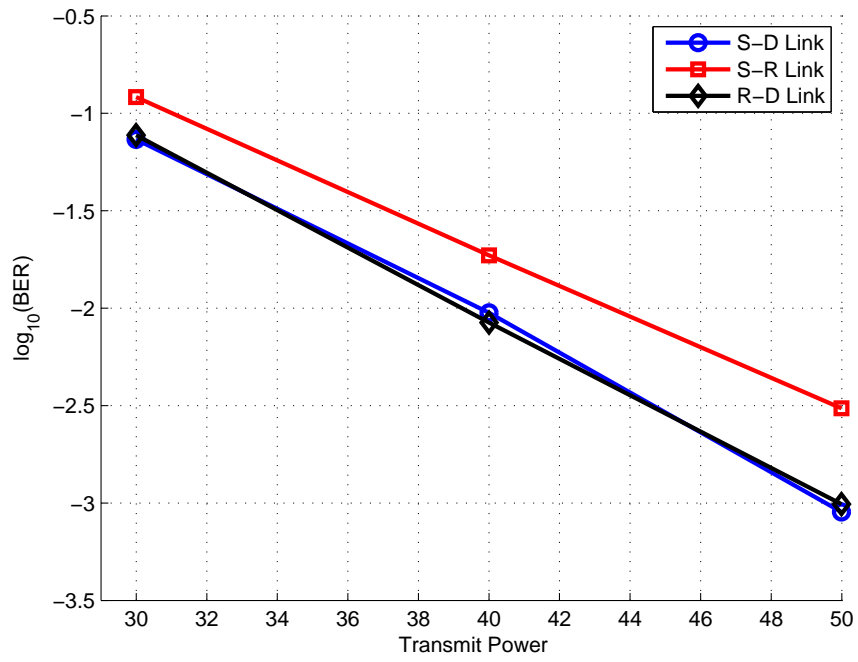


Figure 5.4: BER versus transmit power for three individual links in selective DF relay network

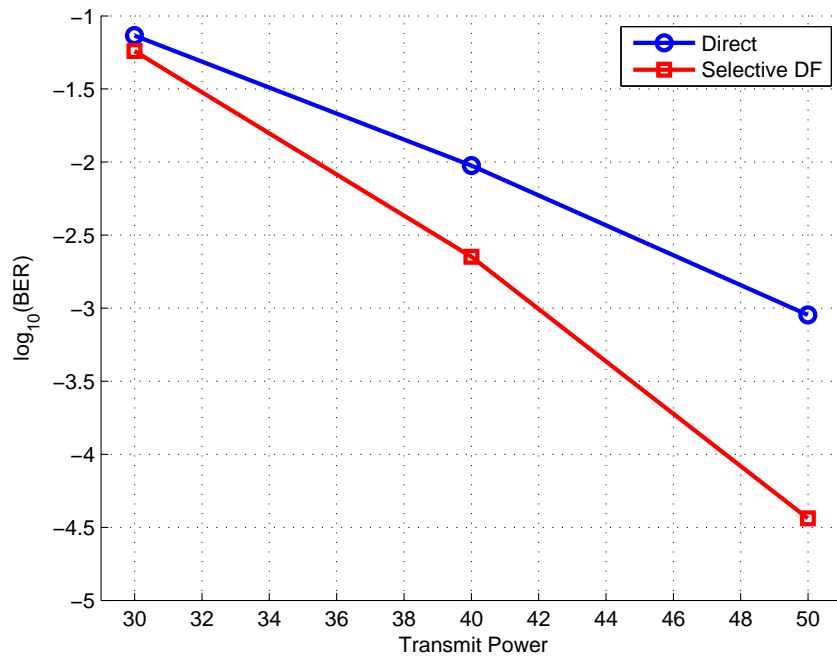


Figure 5.5: BER versus SNR for direct and diversity paths in selective DF relay network

5.5 Summary

For the experimental setup, it was expected to see a steeper decay of the BER curve for the diversity combining scenario. Simulation results indicated that error propagation in the simple DF scheme would negate any diversity gains provided by the system, but by selectively relaying only those packets at the relay that were received without error, the effect of error propagation could be reduced. Experimental data confirmed that the simple DF scheme provided no diversity gain. However, the data showed that by selectively relaying only those packets that are received without error, the system was able to provide a diversity gain. The gain was less than full diversity because the destination did not always receive two copies of the data. The received symbol distribution experiment of the previous chapter cannot prove the presence of a diversity gain, but it can indicate if an underlying requirement for diversity is met, namely an alteration in the instantaneous SNR distribution.

CHAPTER 6

CONCLUSIONS AND FUTURE WORK

This section draws some overall conclusions about the work presented in this thesis and highlights future directions of research.

6.1 Conclusions

Cooperative diversity offers the chance to extend spatial diversity gains achievable with MIMO systems to the distributed setting. Though it is a field that has been analyzed quite thoroughly, there are still very few real world systems that take advantage of the gains cooperative diversity can offer. The primary contribution of this work is the basis for an experimental network to practically evaluate different cooperative communication architectures. This network has the benefit of being developed on open source software, allowing it to be fully utilized and improved on by others. The network was implemented with readily available hardware, making it easy for others to reconstruct.

It is known that diversity gain can be quantified using the instantaneous SNR distribution's behavior around the origin, or equivalently the decay order of the corresponding moment generating function. The instantaneous SNR distribution must therefore differ for direct and diversity transmission. The distribution of received symbols at the destination is dependent on the instantaneous SNR distribution, and therefore also will differ for direct and diversity transmission. Although a change in

distribution alone is not a sufficient guarantee of diversity, it is necessary. Theoretical, simulation, and experimental work all showed that the simple DF scheme was inducing a shift in the distribution of received symbols. We believe this perspective can be useful for protocol development and debugging purposes.

BER curves were obtained for the simple and selective DF diversity schemes. Despite the results from the received symbol distribution section, the simple DF scheme provided no diversity gain due to error propagation at the relay. Selective DF, on the other hand, was able to provide a diversity gain. Although our implementation is not optimal, we believe these results confirm that cooperative transmission can provide diversity benefits in real-world environments and further cooperative protocol development and system architecture.

6.2 Future Work

A natural next step in experimental work with this cooperative transmission implementation is to collect data for different network topologies. Varying the link qualities between nodes can provide data to support theoretical work done to establish for which geometries cooperation is beneficial to an individual and to the network as a whole. Furthermore, data can be collected in different environments, including outside environments, to quantify the usefulness of cooperation for varying degrees of multipath fading.

Additionally, there are various other relaying schemes that have been proposed for use in cooperative communications. Amplify and forward schemes avoid the problem of introducing error propagation at the relay, ensuring that, unlike decode and forward, full diversity is always achieved at the destination. Other schemes use feedback to increase spectral efficiency by only relaying messages when requested. All of these algorithms should outperform the simple DF scheme, but protocol

architecture and ease of implementation would also have to be explored.

Finally, the code developed for these experiments can be improved upon to allow link layer and network layer functionalities to be fully implemented. Many complicated issues and opportunities for improvement exist when considering the mixing of network layer routing and physical layer relaying protocols. These higher layer functionalities will facilitate experimentation and research in cross layer optimization for cooperative schemes.

BIBLIOGRAPHY

- [1] A. Sendonaris, E. Erkip, and B. Aazhang, “User cooperation diversity – part i: System description,” *IEEE Transactions on Communications*, vol. 51, pp. 1927–1938, November 2003.
- [2] A. Sendonaris, E. Erkip, and B. Aazhang, “User cooperation diversity – part ii: Implementation aspects and performance analysis,” *IEEE Transactions on Communications*, vol. 51, pp. 1939–1948, November 2003.
- [3] J. N. Laneman, D. N. C. Tse, and G. W. Wornell, “Cooperative diversity in wireless networks: Efficient protocols and outage behavior,” *IEEE Transactions on Information Theory*, vol. 50, pp. 3062–3080, December 2004.
- [4] A. Scaglione, D. Goeckel, and J. N. Laneman, “Cooperative communications in mobile ad-hoc networks: Rethinking the link abstraction,” *IEEE Signal Processing Magazine*, vol. 23, pp. 18–29, September 2006.
- [5] J. Mitola, “The software radio architecture,” *IEEE Communications Magazine*, pp. 26–38, May 1995.
- [6] “University of notre dame electronic theses & dissertations.” <http://etd.nd.edu/>.
- [7] D. Tse and P. Viswanath, *Fundamentals of Wireless Communication*. Cambridge University Press, June 2005.
- [8] T. Cover and A. E. Gamal, “Capacity theorems for the relay channel,” *IEEE Transactions on Information Theory*, pp. 572–584, September 1979.
- [9] A. Bletsas and A. Lippman, “Implementing cooperative diversity antenna arrays with commodity hardware,” *IEEE Communications Magazine*, pp. 33–40, December 2006.
- [10] P. Murphy, A. Sabharwal, and B. Aazhang, “Building a cooperative communications system.” http://warp.rice.edu/trac/attachment/wiki/JSAC_CooperativeComm/Files/Rice_JSAC_CooperativeComm.pdf?format=raw.
- [11] “Wireless open-access research platform.” <http://warp.rice.edu/index.php>.
- [12] W. H. W. Tuttlebee, “Software-defined radio: Facets of a developing technology,” *IEEE Personal Communications*, pp. 38–44, April 1999.

- [13] S. Haykin, "Cognitive radio: Brain-empowered wireless communications," *IEEE Journal on Selected Areas of Communications*, vol. 23, pp. 201–220, February 2005.
- [14] M. S. Safadi and D. L. Ndzi, "Digital hardware choices for software radio (sdr) baseband implementation," in *Information and Communication Technologies, ICTTA '06*, pp. 2623–2628, April 2006.
- [15] T. Hentschel, M. Henker, and G. Fettweis, "The digital front-end of software radio terminals," *IEEE Personal Communications*, pp. 40–46, August 1999.
- [16] X. Reves, V. Marojevic, R. Ferrus, and A. Gelonch, "Fpga's middleware for software defined radio applications," in *International Conference on Field Programmable Logic and Applications*, pp. 598–601, August 2005.
- [17] "Gnu radio." <http://gnuradio.org/trac/wiki>.
- [18] J. Soulie, "C++ tutorial." <http://www.cplusplus.com/doc/tutorial/>.
- [19] G. van Rossum, "Python tutorial." <http://www.python.org/doc/2.5.2/tut/tut.html>.
- [20] E. Blossom, "Exploring gnu radio." <http://www.gnu.org/software/gnuradio/doc/exploring-gnuradio.html>.
- [21] D. Shen, "Gnu radio tutorials." <https://radioware.nd.edu/documentation>.
- [22] M. Ettus, "Usrc family brochure." http://www.ettus.com/downloads/er_broch_trifold_v5b.pdf.
- [23] D. Shen, "The usrp board." <https://radioware.nd.edu/documentation/hardware-and-usrp/the-usrp-board>.
- [24] M. Ettus, "Usrc transceiver daughterboard brochure." http://www.ettus.com/downloads/transceiver_dbrds_v3b.pdf.
- [25] M. F. Iskander, *Electromagnetic Fields and Waves*. Waveland Press, Inc., 1992.
- [26] G. R. Danesfahani and T. G. Jeans, "Optimisation of modified mueller and muller algorithm," *Electronics Letters*, vol. 31, pp. 1032–1033, June 1995.
- [27] A. Abdi, C. Tepedelenlioglu, M. Kaveh, and G. Giannakis, "On the estimation of the k parameter for the rice fading distribution," *IEEE Communication Letters*, vol. 5, pp. 92–94, March 2001.
- [28] S. Haykin, *Communication Systems*. John Wiley & Sons, Inc., 2001.
- [29] J. Sun and I. Reed, "Linear diversity analyses for m-psk in rician fading channels," *IEEE Transactions on Communications*, pp. 1749–1753, November 2003.
- [30] J. R. Barry, D. G. Messerschmitt, and E. A. Lee, *Digital Communication*. Springer, 2003.

- [31] T. Wang, A. Cano, G. B. Giannakis, and J. N. Laneman, “High-performance cooperative demodulation with decode-and-forward relays,” *IEEE Transactions on Communications*, vol. 55, pp. 1427–1438, July 2007.
- [32] Z. Wang and G. B. Giannakis, “A simple and general parameterization quantifying performance in fading channels,” *IEEE Transactions on Communications*, vol. 51, pp. 1389–1398, August 2003.
- [33] J. N. Laneman and G. W. Wornell, “Energy-efficient antenna sharing and relaying for wireless networks,” in *Proc. IEEE Wireless Communications and Networking Conf. (WCNC)*, pp. 7–12, September 2000.
- [34] D. Chen and J. N. Laneman, “Modulation and demodulation for cooperative diversity in wireless systems,” *IEEE Transactions on Wireless Communications*, vol. 5, pp. 1785–1794, July 2006.